IWMI
International Water
Management Institute

196

Working Paper

Mapping Irrigated and Rainfed Agriculture in Ethiopia (2015-2016) using Remote Sensing Methods

Kiran M. Chandrasekharan, Chandima Subasinghe and Amare Haileslassie

Working Papers

The publications in this series record the work and thinking of IWMI researchers, and knowledge that the Institute's scientific management feels is worthy of documenting. This series will ensure that scientific data and other information gathered or prepared as a part of the research work of the Institute are recorded and referenced. Working Papers could include project reports, case studies, conference or workshop proceedings, discussion papers or reports on progress of research, country-specific research reports, monographs, etc. Working Papers may be copublished, by IWMI and partner organizations. Although most of the reports are published by IWMI staff and their collaborators, we welcome contributions from others. Each report is reviewed internally by IWMI staff. The reports are published and distributed both in hard copy and electronically (www.iwmi.org) and where possible all data and analyses will be available as separate downloadable files. Reports may be copied freely and cited with due acknowledgment.

About IWMI

The International Water Management Institute (IWMI) is an international, research-for-development organization that works with governments, civil society and the private sector to solve water problems in developing countries and scale up solutions. Through partnership, IWMI combines research on the sustainable use of water and land resources, knowledge services and products with capacity strengthening, dialogue and policy analysis to support implementation of water management solutions for agriculture, ecosystems, climate change and inclusive economic growth. Headquartered in Colombo, Sri Lanka, IWMI is a CGIAR Research Center and leads the CGIAR Research Program on Water, Land and Ecosystems (WLE). www.iwmi.org

IWMI Working Paper 196

Mapping Irrigated and Rainfed Agriculture in Ethiopia (2015-2016) using Remote Sensing Methods

Kiran M. Chandrasekharan, Chandima Subasinghe and Amare Haileslassie

International Water Management Institute (IWMI)
P. O. Box 2075, Colombo, Sri Lanka

The authors:
Kiran M. Chandrasekharan is a GIS/RS Specialist at the International Water Management Institute (IWMI), Colombo, Sri Lanka; Chandima Subasinghe is a GIS/RS Analyst at IWMI, Colombo, Sri Lanka; and Amare Haileslassie is a Principal Researcher at IWMI, Addis Ababa, Ethiopia.

Chandrasekharan, K. M.; Subasinghe, C.; Haileslassie, A. 2021. *Mapping irrigated and rainfed agriculture in Ethiopia (2015-2016) using remote sensing methods*. Colombo, Sri Lanka: International Water Management Institute (IWMI). 31p. (IWMI Working Paper 196). doi: https://doi.org/10.5337/2021.206

/ irrigated farming / rainfed agriculture / mapping / remote sensing / irrigated land / farmland / water management / biomass / dry season / moisture content / land cover / satellite imagery / landsat / weather data / rainfall patterns / datasets / normalized difference vegetation index / moderate resolution imaging spectroradiometer / time series analysis / Ethiopia /

ISSN 2012-5763
e-ISSN 2478-1134
ISBN 978-92-9090-913-2

Please send inquiries and comments to IWMI-Publications@cgiar.org

A free copy of this publication can be downloaded at:
https://www.iwmi.org/publications/iwmi-working-papers/

Acknowledgments

The authors would like to thank Jennie Barron (Professor - Agricultural Water Management, Department of Soil and Environment, Swedish University of Agricultural Sciences [SLU], Uppsala, Sweden; formerly Strategic Program Leader - Building Resilience, International Water Management Institute [IWMI]) for initiating this work. The Directorate of Small-scale Irrigation at the Ministry of Agriculture and members of the Agricultural Water Management Platform in Ethiopia are also acknowledged for their constructive comments during the conceptualization of this review.

Project

This study was undertaken as part of the *Resilience and sustainability through small-scale irrigation intensification* project, which is mapped to Flagship 2 - Land and Water Solutions for Sustainable Agriculture (LWS) of the CGIAR Research Program on Water, Land and Ecosystems (WLE).

Donors

This research was carried out as part of the CGIAR Research Program on Water, Land and Ecosystems (WLE) and supported by Funders contributing to the CGIAR Trust Fund (https://www.cgiar.org/funders/).

Contents

Acronyms and Abbreviations

CART	Classification and Regression Tree
CHIRPS	Climate Hazards group InfraRed Precipitation with Stations
DEM	Digital Elevation Model
EVI	Enhanced Vegetation Index
FAO	Food and Agriculture Organization of the United Nations
GMIA	Global Map of Irrigated Areas
GPS	Global Positioning System
HDF	Hierarchical Data Format
IWMI	International Water Management Institute
MoA	Ministry of Agriculture
MoANR	Ministry of Agriculture and Natural Resources
MODIS	Moderate Resolution Imaging Spectroradiometer
MoWIE	Ministry of Water, Irrigation and Energy
NASA	National Aeronautics and Space Administration
NDMI	Normalized Difference Moisture Index
NDVI	Normalized Difference Vegetation Index
NIR	Near Infrared
OIDA	Oromia Irrigation Development Authority
OLI	Operational Land Imager
QA	Quality Assessment
SAR	Synthetic Aperture Radar
SNNPR	Southern Nations, Nationalities, and People's Region
SRTM	Shuttle Radar Topography Mission
SWIR	Short-wave Infrared
TIRS	Thermal Infrared Sensor
TOA	Top of Atmosphere
USGS	United States Geological Survey
WRS	Worldwide Reference System

Summary

Irrigation expansion is a critical development intervention to address food security challenges in Ethiopia. However, only a fraction of the country's irrigation potential has been utilized thus far. Enhanced spatial information on irrigated land can support policy and practice by making agricultural land and water management solutions more effective. Currently, considerable variations exist in the irrigated area estimations undertaken by different government agencies. Furthermore, the irrigated area maps developed as part of global mapping efforts are too coarse for planning and management at the subnational scale. This study aims to develop an irrigated area map of Ethiopia using satellite images to support agricultural water management practices in the country, using multi-temporal, multi-resolution data sets from 2015 to 2016.

The identification of irrigated areas was achieved by analyzing seasonal changes in the biomass and dry season moisture status of agricultural areas. As an initial step, a country-wide agricultural area map was developed using Landsat 8 images to remove non-agricultural land cover types. Subsequently, the seasonal changes in the agricultural areas were analyzed with an annual time series of Moderate Resolution Imaging Spectroradiometer (MODIS) 16-day maximum Normalized Difference Vegetation Index (NDVI) composite data, along with Climate Hazards group InfraRed Precipitation with Stations (CHIRPS) rainfall time series for the same period. Landsat 8 data were used to analyze the dry season moisture status.

The classification was carried out by combining the temporal correlation of crop growth patterns with rainfall, the number of crop cycles in a year and dry season moisture status. The seasonal variables were derived by Fourier analysis and a time-lagged regression. The dry season moisture index was captured through the Normalized Difference Moisture Index (NDMI) data developed using Landsat 8 data.

The study resulted in a map of irrigated and rainfed areas with a spatial resolution of 30 m. The total area of croplands was estimated as 21.8 million hectares (Mha), of which only 1.11 Mha were mapped as the irrigated area. This is only around 5% of the estimated total agricultural area. Validation using the geographic coordinates of irrigated areas obtained from the records of the Ministry of Agriculture (MoA) in Ethiopia showed an agreement of 70% with the results of this study. The results broadly match the recent estimations by MoA based on field information. A comparison of the results with the area estimations by the government agencies is also provided.

This study provides the spatial extent and distribution of existing irrigated areas, which can strengthen future efforts to monitor irrigation development in Ethiopia. Further work on irrigation suitability analysis combined with the results of this study can also provide valuable information for decision-makers and investors about future irrigation development in the country.

Mapping Irrigated and Rainfed Agriculture in Ethiopia (2015-2016) using Remote Sensing Methods

Kiran M. Chandrasekharan, Chandima Subasinghe and Amare Haileslassie

Introduction

Ethiopia is the second-most populous country in Africa after Nigeria and is one of the fastest-growing economies in the region. However, it remains one of the poorest countries in the world. Agriculture is the mainstay of the economy, accounting for ~85% of the labor force (Welteji 2018). Irrigation expansion is considered critical to increasing agricultural productivity and is consequently of high priority to sustainably intensify agriculture and improve food security (Schmitter et al. 2018). However, only a small portion of the country's irrigation potential is utilized so far (Worqlul et al. 2017).

Information about the location and spatial extent of the irrigated as well as rainfed areas is an important requirement for sustainable water resources development and agricultural planning. However, reliable estimates of the geographical extent and maps of irrigated areas are not available for most of Ethiopia. Information about the areal extent of irrigation is collected by various government agencies in Ethiopia. However, major differences exist in the statistics reported (MoWIE 2018; Haile and Kassa 2015). Countrywide maps of irrigated areas are primarily available through various global mapping efforts such as the Global Map of Irrigated Areas (GMIA) (Siebert et al. 2013a, 2013b) published by the Food and Agriculture Organization of the United Nations (FAO), and the Irrigated and Rainfed Area Map of Africa (Chandrasekharan et al. 2015). The FAO GMIA primarily uses the area statistics reported by the government and other national or international agencies; it expresses the irrigated area as a percentage of a grid cell of approximately 10 km x 10 km resolution. For Ethiopia, FAO mainly uses the statistics reported for the year 2001 with some areas updated with statistics from 2004 (FAO 2016). The Irrigated and Rainfed Area Map of Africa (Chandrasekharan et al. 2015) is based on satellite images with 250 m resolution acquired during the period 2010-2011. The area estimation based on this map has disparities, generally overestimation, as compared with the statistics reported by the government as well as popular perception.

Most global maps apply generalized classification rules developed for large regions, which would increase the uncertainties at a local scale. The coarse pixel resolutions also contribute to the uncertainty due to the mixed land cover at sub-pixel resolutions present in most Ethiopian agricultural landscapes. An important prerequisite for the irrigated/rainfed categorization of agricultural areas is information about the spatial extent of croplands corresponding to the study period at an appropriate resolution. Most crop area maps of Ethiopia available in the public domain are from various global land cover mapping products such as GlobCover, Moderate Resolution Imaging Spectroradiometer (MODIS) land cover, etc. While most of these coarse-resolution products are successful in capturing large continuous agricultural areas, they generally fail to map fragmented agricultural areas and misclassify significant areas of non-crop land cover as crop cover. Because of the coarse resolution of these maps, the smaller non-agricultural areas within the croplands, such as natural vegetation patches, hamlets, smaller grasslands, etc., are usually misclassified as agricultural land. The inclusion of wetlands or evergreen vegetation in agricultural areas eventually leads to the misclassification of such areas into irrigated areas. Therefore, it was essential for this study to develop a more accurate crop area map of the study area to avoid potential large-scale overestimation of irrigated areas.

This study aimed to develop a map of irrigated and rainfed areas of Ethiopia using remote sensing data. As an important prerequisite for the irrigated/rainfed categorization, an agricultural area map had to be prepared. The study aimed to develop an agricultural area map and irrigated area identification using satellite images from 2015 to 2016, and provide area estimations at subnational levels.

Materials and Methods

The analysis was performed in two stages. Irrigated and rainfed areas were mapped by analyzing seasonal trends in vegetation biomass and dry season moisture status in agricultural areas. Many non-agricultural land cover types such as forests and wetlands have spectral and seasonal characteristics similar to agricultural lands. As an initial step, an agricultural area map was developed excluding such areas. The agricultural areas identified by this map were further classified as irrigated and rainfed in the subsequent analysis.

Remotely sensed images over multiple dates were used for the preparation of the agricultural area map. The mapping of irrigated and rainfed areas in the areas identified as croplands was undertaken by utilizing time series data sets of vegetation indices and satellite-derived rainfall data sets. Apart from the original spectral bands, various spectral indices derived from the imagery were also used for the analysis at various stages. Furthermore, the analysis was supported by ground truth information obtained through field surveys, secondary sources and visual interpretation of high-resolution images.

Spectral Indices for Classification

The use of spectral indices derived through different satellite image band combinations is a common practice in remote sensing analysis. Spectral indices used for mapping of agricultural and irrigated areas in this study are described below.

Normalized Difference Vegetation Index (NDVI): NDVI is probably the most frequently used vegetation index derived from remote sensing data. It is strongly correlated with many vegetation parameters such as crown closure, leaf vigor, canopy biomass and leaf area index (Lyon et al. 1998). NDVI is derived from the red (R) and near infrared (NIR) bands of the satellite images using the following formula:

$$NDVI = \frac{(\rho_{NIR} - \rho_{R})}{(\rho_{NIR} + \rho_{R})} \quad \ldots\ldots\ldots\ldots\ldots\ldots\ldots \quad (1)$$

where: ρ_R is the red band reflectance and ρ_{NIR} is the near infrared band reflectance.

NDVI has been successfully used for mapping and monitoring vegetation, including land use and irrigated area mapping at multiple scales, often along with original spectral bands and other spectral indices (Dahal et al. 2018; Pervez et al. 2014; You et al. 2013; Thenkabail and Wu 2012; Thenkabail et al. 2009). NDVI is less affected by various forms of illumination, and atmospheric and topographic effects due to its ratio properties (Matsushita et al. 2007; Huete et al. 2002). However, NDVI values tend to saturate in areas with high biomass; as a result, differentiation of dense vegetation types based on NDVI will be constrained by index saturation at higher values (Huete et al. 2002; Pun et al. 2017; Naser et al. 2020). Enhanced Vegetation Index (EVI), which is free from the saturation effect, is often proposed as an alternative to NDVI. However, EVI is highly susceptible to the topographic effects (Matsushita et al. 2007) and may not be suitable for many areas of Ethiopia due to the mountainous terrain.

The impact of NDVI saturation is most visible during the period with peak biomass, whereas NDVI during the growing season is not affected by the saturation (Matsushita et al. 2007; Huete et al. 2002). It has also been observed that NDVI has a higher range in values over the semiarid areas, but this is at the expense of a lower dynamic range over the more humid forested sites (Huete et al. 2002). An evaluation of seasonal trends in NDVI in several crop types showed that NDVI is suitable for distinguishing the vegetation categories during the growing period, which indicates that the multi-temporal NDVI data are suitable for differentiating vegetation categories (Wardlow et al. 2007).

If the vegetation classification is solely based on NDVI, the saturation effect would lead to limited success in distinguishing areas with dense forests from certain irrigated areas or identifying various irrigated crop types during the peak of the growth. However, it has been observed that the use of functionally different indices increases classification proficiency (Pun et al. 2017). In this analysis, multi-temporal NDVI has been used along with other spectral bands, spectral indices and topographic variables to map the crop areas. A time series of NDVI along the entire crop cycle was used for further classification of irrigated and rainfed areas.

Normalized Difference Moisture Index (NDMI): NDMI value is an indicator of the moisture levels stored in vegetation. The index is derived based on the absorption of water by the short-wave infrared (SWIR)-1 band compared to the NIR band (Wilson and Sader 2002; USGS 2016). NDMI was derived from the NIR and SWIR bands of Landsat 8 using the following formula:

$$NDMI = \frac{(\rho_{NIR} - \rho_{SWIR\,1})}{(\rho_{NIR} + \rho_{SWIR\,1})} \quad \ldots\ldots\ldots\ldots\ldots\ldots\ldots \quad (2)$$

where: ρ_{NIR} is the near infrared band reflectance and $\rho_{SWIR\,1}$ is the short-wave infrared -1 band reflectance.

Although the biophysical interpretation of indices that use the SWIR band is more ambiguous than indices that use only red and NIR bands (Wilson and Sader 2002), they seem to account for moisture content in vegetation and soil.

NDMI was used at both stages of the analysis. Multi-temporal NDMI was used as one of the input layers for the

crop area classification. The index was further used for the identification of irrigated areas in the subsequent stage of the analysis.

Data Sources

The analysis was performed using publicly available, free satellite data sets along with geographical coordinates of irrigated areas obtained through primary field surveys and secondary data sets. Satellite images acquired at regular intervals over one year were used to analyze the seasonal trends. An annual time series of MODIS 16-day NDVI maximum value composite data were used to capture the seasonal variation of vegetation. Landsat 8 images were used for mapping the agricultural areas and assessing the dry season moisture status in croplands. The analysis was supported by global open access rainfall data sets and crop area maps. The characteristics of these data sets and use of the data are described below.

Landsat 8

Landsat 8 images were used to prepare the crop area map and further analyze the irrigation status of the crop areas. Landsat 8 images have 11 spectral bands including one panchromatic and two thermal bands. The panchromatic band has a spatial resolution of 15 m. The thermal bands are acquired with a 100 m resolution but are resampled to 30 m in the delivered data product. The other bands have a resolution of 30 m. Additionally, a Quality Assessment (QA) band, which provides information about the cloud cover and cloud shadows, is also available for Landsat 8 data. The panchromatic band was not used for the analysis. Thus, the analysis involving Landsat 8 images was carried out at 30 m resolution.

Two different Landsat 8 data products were used for this study. The crop area classification was performed using the Landsat 8 Collection 1 Tier 1 8-Day Top of Atmosphere (TOA) Reflectance Composite imagery available in Google Earth Engine.[1] These mosaics are created from all the scenes in each eight-day period beginning from the first day of the year (Google Earth Engine 2017). Spectral indices for the analysis of irrigation status of the agricultural areas were derived using the Landsat 8 Operational Land Imager/ Thermal Infrared Sensor (OLI/TIRS) Surface Reflectance product available from the United States Geological Survey (USGS) Earth Explorer[2] satellite data archive (USGS 2016). The geographical area of Ethiopia is covered by 59 Landsat 8 scenes (Figures 1 and 2). The satellite images acquired between January 2015 and September 2016 were used at various stages of the analysis. Images of the same period were not available for the entire country because of cloud cover. Scenes with more than 20% cloud cover were not used for the analysis. Multi-season images for each scene were used for the classification to reduce the impact of clouds.

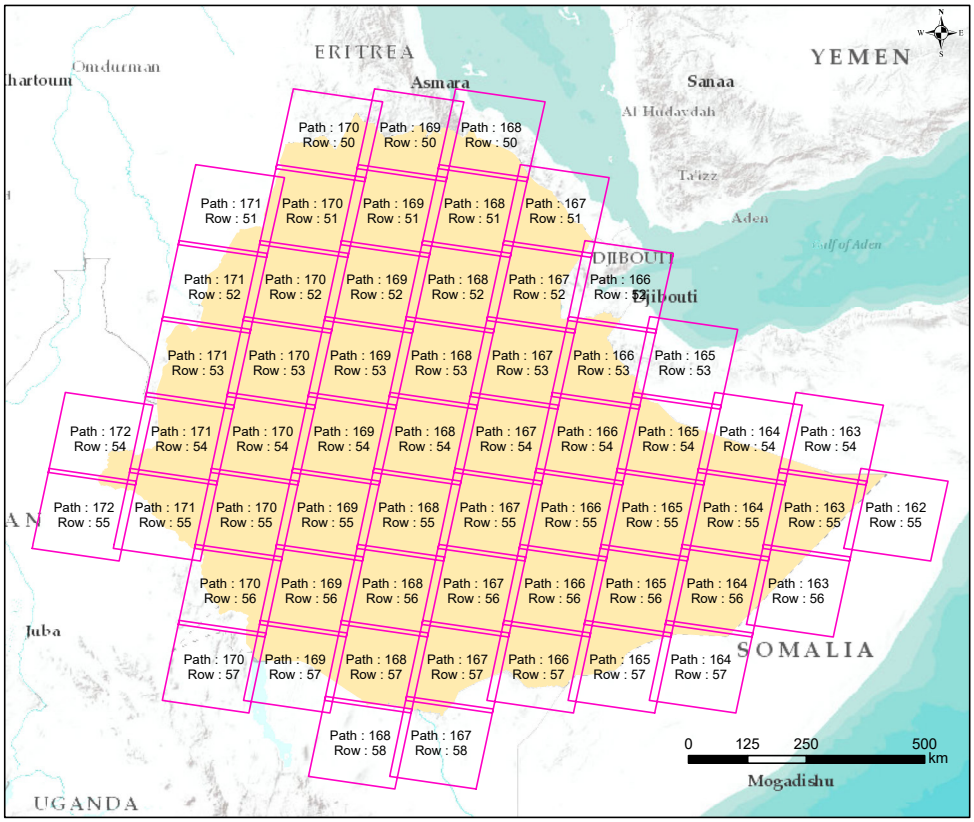

Figure 1. Landsat 8 scene footprints of Ethiopia, according to the Landsat Worldwide Reference System 2 (WRS 2).

[1] https://earthengine.google.com/
[2] https://earthexplorer.usgs.gov/

MODIS NDVI

The identification of irrigated and rainfed areas within the agricultural landscape was carried out through a time series analysis of intra-annual vegetation indices. The MODIS NDVI data product MOD13Q1 was used to represent the seasonal changes in vegetation. The MOD13Q1 NDVI data set is a 16-day maximum value composite derived from daily satellite data (Didan 2015) with a spatial resolution of 250 m. The time series image data set for this study was developed from the MOD13Q1 data products from April 2015 to March 2016. Four MODIS scenes were required to cover Ethiopia, and for each scene, 23 images were required to create the time series data set for the study period. The MODIS data set distributed by USGS through the National Aeronautics and Space Administration (NASA) Earthdata Search[3] system was used. The data set is available with sinusoidal projection in Hierarchical Data Format (HDF). The images downloaded were converted to ERDAS Imagine format and re-projected to the geographic (latitude/longitude) coordinate system.

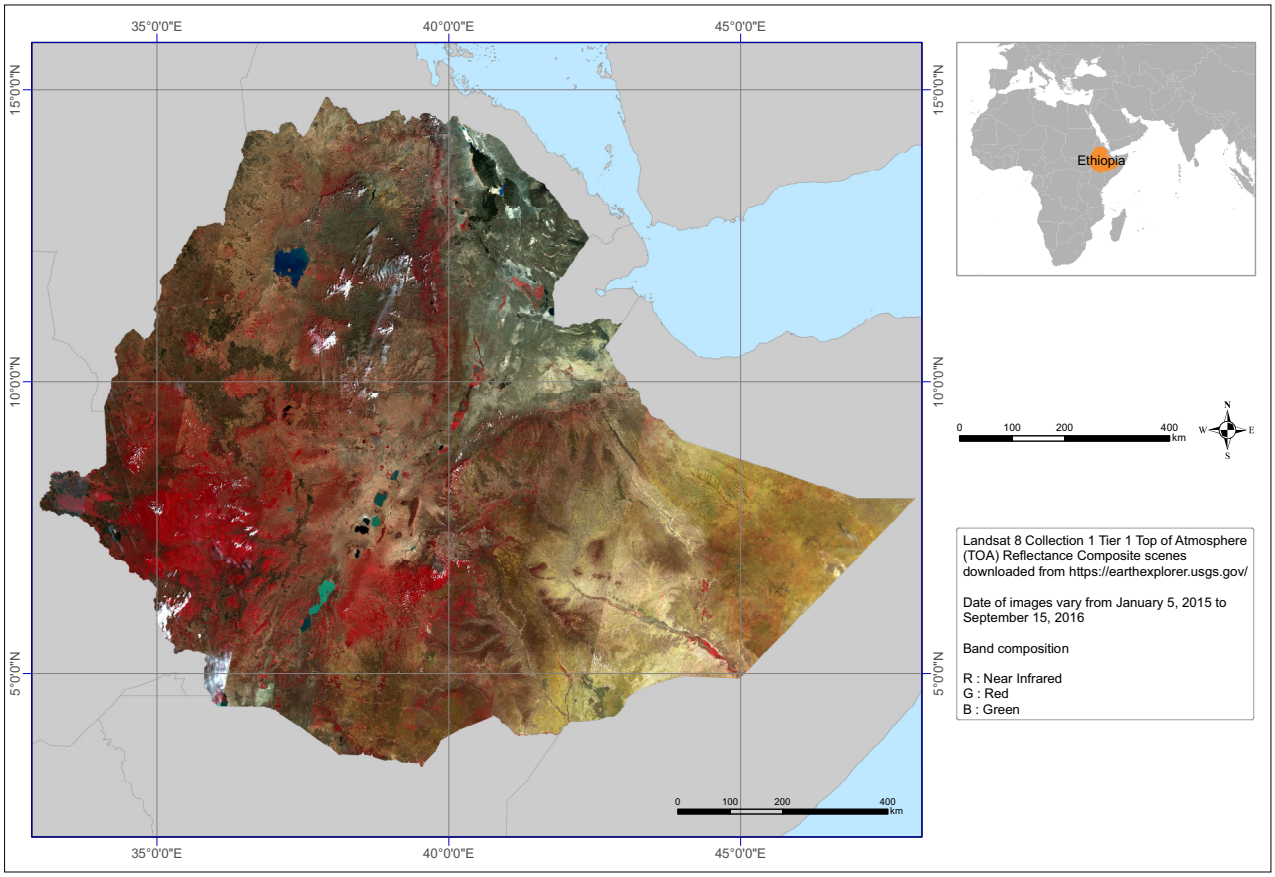

Figure 2. Mosaic of Landsat 8 scenes of Ethiopia.

Climate Hazards group InfraRed Precipitation with Stations (CHIRPS) Rainfall Data

An annual time series of rainfall data was also used along with the vegetation/NDVI images to analyze the seasonal changes. Daily global rainfall images of the Climate Hazards group InfraRed Precipitation with Stations (CHIRPS) were downloaded from the website of the Climate Hazards Centre[4] (Funk et al. 2015). The spatial resolution of the data is 0.05° or 5 km (approximately). A 16-day rainfall time series corresponding to each 16-day NDVI composite was created from the daily rainfall data to match the temporal resolution of the MODIS NDVI data series.

Ground Truth Data

Geographic coordinates of sample locations for this study were obtained through field surveys, high-resolution images in the Google Earth platform,[5] and from past studies and government records.

[3] https://search.earthdata.nasa.gov/
[4] https://data.chc.ucsb.edu/products/CHIRPS-2.0/
[5] https://search.earthdata.nasa.gov/

Field data collection: Geographical coordinates of irrigated and rainfed areas were collected from different parts of the country using a hand-held global positioning system (GPS). The survey was conducted in 2017. Coordinates were collected from within plots with relatively uniform land use. Additionally, the survey team interacted with field-level officials from the Ministry of Agriculture (MoA) at different locations to gather descriptive information about irrigation patterns and extents. GPS coordinates collected for earlier projects of the International Water Management Institute (IWMI) in 2010 and 2015 were also used. The data collected during 2015 and 2017 were used for the irrigated and rainfed area classification of agricultural areas. The 2010 data were used for validation as the irrigation status of those locations has not changed over the years.

Google Earth images: Sample locations for the crop area classification were obtained through visual interpretation of the high-resolution (up to 0.65 m) images available in the Google Earth platform. Google Earth images were also used for visual cross-verification and correction of the classification results. Although the images are of high resolution, it is often not possible to determine the irrigation status of crops using Google Earth alone. Therefore, this resource was not used for the irrigated-rainfed classification of agricultural areas.

Coordinates from secondary sources: Coordinates of irrigated areas from several locations in the Oromia and Tigray regions were available from the records of MoA. Additionally, irrigated site polygons digitized over Google Earth imagery were available for two districts of the Southern Nations, Nationalities, and People's Region (SNNPR). These data sets were used for both the classification and validation of the results.

Detailed metadata of these data sets were not available. The Oromia ground truth data set was generated through partial site visits and secondary data available at the district level from past surveys or studies (OIDA 2018). Data collection methods used for other data sets are not available at the time of writing this report.

The classification of remote sensing images and validation of results require GPS coordinates collected from within the plots to enable pixel-to-pixel comparison. Ideally, the coordinates should be obtained from areas with relatively uniform land cover. Location coordinates collected for other purposes often do not meet this quality criterion. The available coordinates from the secondary sources were plotted on Google Earth images and were visually verified for their suitability for the use in the classification and validation. Some of the points seem to have been taken at adjacent locations of agricultural lands, presumably from an easily accessible location or at the diversion/abstraction location of the irrigation scheme. Wherever the irrigated areas represented by those points could be clearly identified visually, these points were manually moved to the irrigated area. Since the modified locations are visually interpreted data, these were used only for the purpose of classification and were not included in the validation data set.

Crop Area Mapping

The crop area map of Ethiopia was prepared as an initial step to exclude the non-agricultural areas from the analysis. The mapping was carried out using the satellite data archives and classification procedures available in Google Earth Engine. Google Earth Engine is an advanced, cloud-based geospatial processing platform facilitating access to a wide range of raw and derived satellite data products and classification algorithms. The classification was performed using the Landsat 8 Collection 1 Tier 1 8-day TOA Reflectance Composite imagery as input (as mentioned in the section *Data Sources*). An initial classification with single date imagery for a sample area did not produce the desired result. The separation of cultivated savannah and bushlands from natural savannah and bushlands was particularly challenging. However, the seasonal changes occurring in cultivated areas and natural vegetation are likely to be different in most situations. These changes can be captured through images acquired on multiple dates for each scene and can be used as input to improve the classification (Krishnaswamy et al. 2004; Senf et al. 2015). In addition to the original bands from the multi-seasonal images, spectral indices such as NDVI, NDMI and topographic data sets were also used for the classification (Morton and Rowland 2015). The list of Landsat scenes and the dates of the images used for the classification of crop areas are shown in Table 1. An overview of the classification process is presented in Figure 3.

Table 1. List of Landsat 8 scenes and dates of the images used for the crop area classification according to the Landsat WRS 2.

		Row								
		50	51	52	53	54	55	56	57	58
Path	162						Jan 14, 2016			
	163					Jan 21, 2016				
	164					Jan 12, 2016				
	165				Jan 19, 2016 / Sep 15, 2016					
	166			Feb 11, 2016						
	167		Jan 14, 2015 / Feb 18, 2016 / March 5, 2016 / Mar 21, 2016							
	168	Jan 8, 2016/Jan 24, 2016/ Mar 12, 2016/ Mar 28, 2016			Jan 5, 2015 / Feb 6, 2015 / Jan 24, 2016 / Mar 28, 2016				Feb 6, 2015 / Jan 24, 2016	
	169	Jan 28, 2015 / Jan 15, 2016 / Feb 16, 2016 / Mar 3, 2016					Jan 28, 2015			
	170	Jan 22, 2016 / Feb 7, 2016 / Feb 23, 2016 / Mar 10, 2016						Jan 22, 2016 / Feb 7, 2016 / Feb 23, 2016 / Mar 10, 2016		
	171		Jan 13, 2016 / Feb 14, 2016							
	172					Jan 20, 2016				

Beyond the Ethiopian country boundary

The following data set was constructed for each Landsat 8 scene as the classification input.

- *Bands 1 to 7 of multi-date images from Landsat 8 sensor:* The images were selected from the period January 2015 to September 2016. The number and dates of images used for each scene are different due to the availability of cloud-free images. The images that were least affected by the clouds were selected as inputs for each scene. The clouds and cloud shadows of the selected images were removed using masks generated from the Landsat 8 QA band. Since the analysis used images from multiple seasons, cloud-free pixels from at least one of the selected dates were available for the cloud-masked areas.
- *NDVI:* Derived for each of the Landsat 8 images selected for the analysis.
- *Mean NDVI:* Mean value of the NDVI data from multiple dates selected for the analysis.
- *Standard Deviation of NDVI:* Derived from the NDVI of multiple dates selected for the analysis.
- *NDMI:* Derived for each of the Landsat 8 images selected for the analysis.
- *Mean NDMI:* Mean value of NDMI data from multiple dates selected for the analysis.
- *Altitude:* From Shuttle Radar Topography Mission (SRTM) Digital Elevation Model (DEM) with 30 m resolution (NASA JPL 2013)
- *Slope:* Derived from the SRTM DEM.

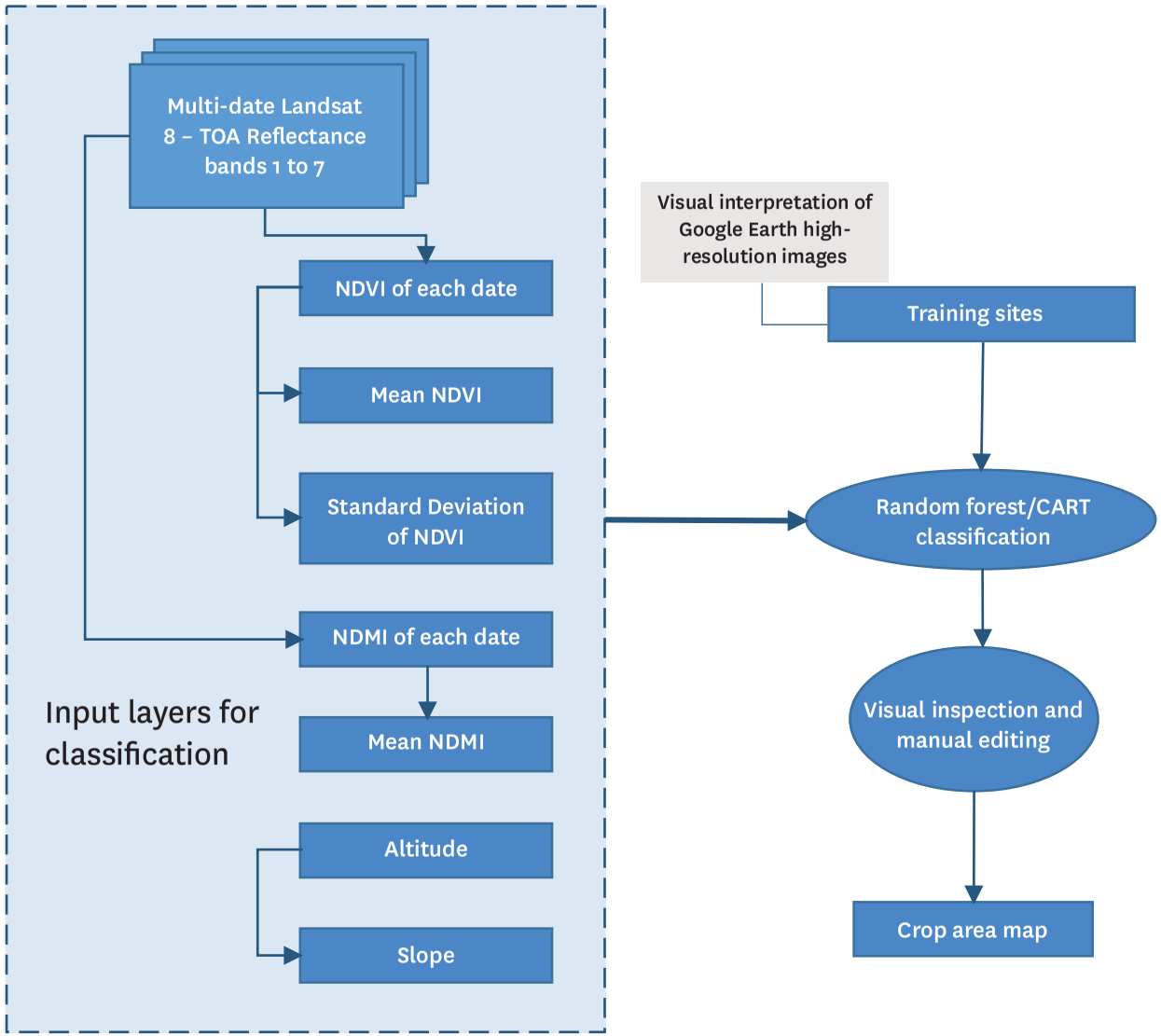

Figure 3. Overview of the crop area mapping process using Landsat 8 images.

Notes: TOA - Top of Atmosphere; NDVI - Normalized Difference Vegetation Index; NDMI - Normalized Difference Moisture Index; CART - Classification and Regression Tree.

Even though the objective was to develop a crop area map, all major land cover categories had to be included in the classification process to avoid possible misclassification of various land cover types as an agricultural category due to spectral reflectance similarities to croplands. The signatures for classification were developed for several subcategories of croplands, such as standing crops, harvested/fallow lands, agricultural plantations, woodlands with cultivation and bushlands with cultivation, and nonagricultural land uses, such as forest, woodland, dense bushland, bushland, grassland, bare land, marshland, water and urban areas. The signatures were developed from training samples selected from the high-resolution images available through the Google Earth Engine interface. The training samples, selected from the areas where the respective land use is prominent, were spatially well distributed over the map region. The primary purpose of developing signatures for non-agricultural classes is to provide a suitable category to accommodate the pixels belonging to those classes to avoid them being misclassified as agriculture. Hence, the fine distinction between those categories was not addressed for the development of signatures and the remaining classification process.

We used both Random Forest Classification and Classification and Regression Tree (CART) algorithms for the classification of the input data set. Parametric classification approaches such as Maximum Likelihood Classification are often less efficient in heterogeneous landscapes, where it is difficult to obtain a sufficient number of normally distributed sample locations. Non-parametric approaches, such as CART (Breiman et al. 1984), and ensemble learning algorithms, such as Random Forests (Breiman 2001), have been producing better results for such landscapes. The Random Forests method is considered to be one of the most effective algorithms for satellite image classification (Iverson et al. 2008).

The classification outputs were visually compared with the high-resolution images and the more accurate results were selected for further processing. The results were downloaded from the Google Earth Engine as tiles with 30 m spatial resolution. The output layers were compared with high-resolution images available in Google Earth and manually edited to improve the accuracy of agriculture categories. The tiles were mosaiced and a 3 x 3 majority filter was used to remove the image speckle in the output map known as salt and pepper noise effect resulting from high local heterogeneity in pixel values (Ouma and Tateishi 2008). Finally, the non-agricultural classes were removed to create the crop area map.

Classifying Irrigated and Rainfed Areas

The agricultural areas were further classified into irrigated and rainfed areas. Conventional methods of satellite image classification heavily rely on the spectral reflectance properties or signatures of distinct land use and land cover types. The spectral signatures derived from multispectral satellite data for the irrigated and rainfed areas did not show significant differences to enable segregation of these two categories. However, the rainfed and irrigated areas did exhibit significant dissimilarities in the intra-annual changes in green biomass. The growth and decline of green vegetation in rainfed areas are closely linked with the rainfall season, while the changes in irrigated areas show less temporal correlation with the rainfall season. It was also noticed that the moisture levels captured through spectral indices during the dry season are higher in irrigated areas compared to rainfed areas. The irrigated area identification was achieved by analyzing the seasonality properties and dry season moisture status.

Analysis of Seasonality

Time series analysis of annual NDVI and rainfall data was used to explore the seasonal changes and the temporal correlation of the growth/decline cycle of green biomass in agricultural areas to differentiate/identify irrigated and rainfed areas. The period for the time series data definition and analysis was determined according to the annual crop calendar of Ethiopia. While there are regional differences in the rainfall pattern, the major rainfall season for most regions of Ethiopia begins from May/June and continues until August/September. Accordingly, the major cropping season also begins during this period for most of the country. Some areas receive a second rainfall during March/April, and many such areas have a second cropping season too. Thus, the crop calendar year for this analysis was defined as April 2015 to March 2016 to ensure that it covers the major crop cycles in most parts of Ethiopia.

The 16-day MODIS NDVI and CHIRPS rainfall data sets, as described earlier, were used to create the time series data sets for this period. We assumed the relationship between rainfall patterns and seasonal changes in vegetation to be different for irrigated and rainfed agriculture. The NDVI and rainfall trends of several locations were explored to understand the differences in the patterns of biomass change between irrigated and rainfed areas. These locations were selected based on available ground truth information from various sources described earlier.

As evident from the NDVI-rainfall profile plots (Figures 4 and 5), both rainfed and irrigated areas exhibit significantly different temporal relationships with the rainfall patterns. Irrigated area profiles were developed from sample locations identified using a subset of available geographic coordinates. Locations for the rainfed crop trends were identified through visual interpretation of Google Earth images. These locations were mostly dry season fallows, which are most likely rainfed areas in the Ethiopian context. The growth and decline of green vegetation in rainfed areas closely follow

the rainfall pattern of those areas. Since the irrigated areas do not directly depend on the rainfall patterns of the area, these areas show less correspondence with the rainfall patterns.

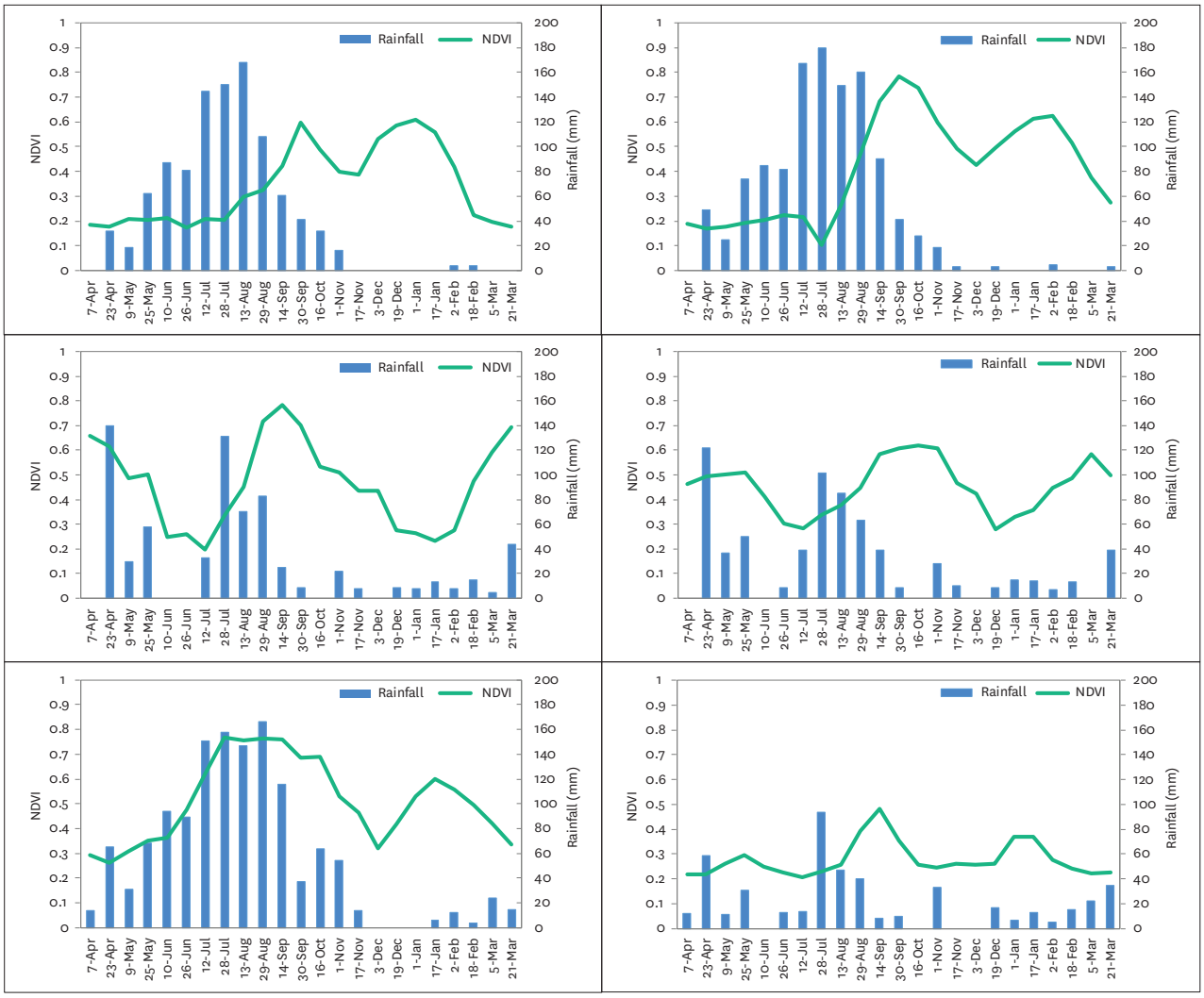

Figure 4. Examples of NDVI and rainfall trends in irrigated areas identified through field surveys.
Note: NDVI = Normalized Difference Vegetation Index.

The NDVI—rainfall trends and the information about the crop calendar and irrigation patterns gathered from various sources show that the following characteristics would be useful to distinguish between irrigated and rainfed areas:

- Most irrigated areas have multiple crop cycles in a year, whereas most rainfed areas have only one crop cycle per year. However, since some areas have a second crop cycle utilizing the remaining moisture of the first crop season or having a second rainfall season, the number of crop cycles alone cannot be used as an identifier of irrigated areas.
- A second or third crop during the January—March period indicates a higher probability of irrigated areas.
- Vegetation growth periods in rainfed areas have high temporal correspondence with the rainfall season. This correspondence is much weaker in irrigated areas.

Both the NDVI and rainfall data sets for the period were analyzed using the time series analysis techniques. Fourier analysis was used to analyze the crop cycle frequency while time-lagged regression techniques were used to analyze the NDVI-rainfall relationships. Figure 6 provides an overview of the data inputs and classification methods used for identifying irrigated and rainfed areas.

Fourier Analysis

The seasonal vegetation change in agricultural areas follows a cyclic nature over time. The green biomass in crop areas gradually increases during the growing

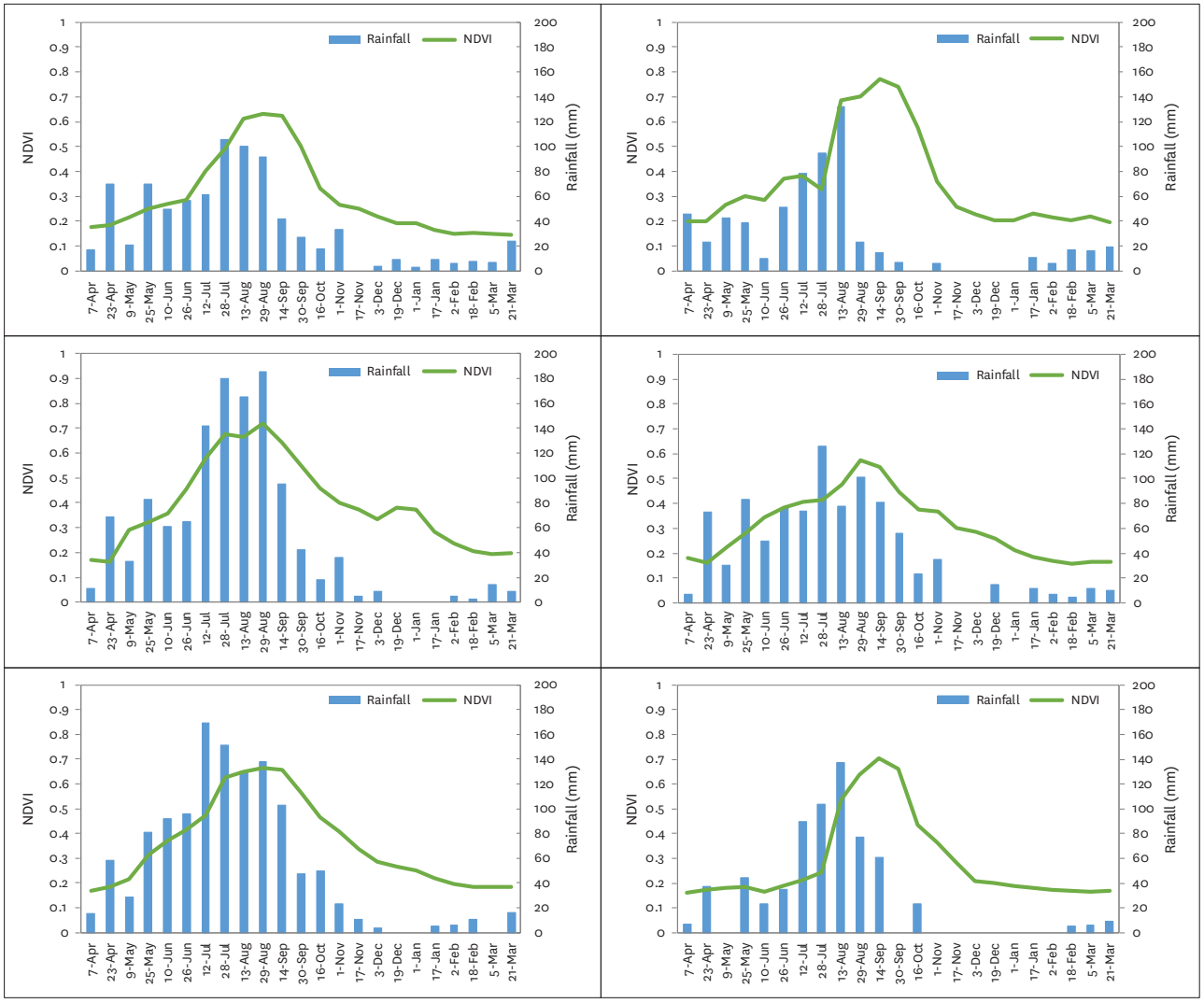

Figure 5. Examples of NDVI and rainfall in potentially rainfed areas identified through visual interpretation.

season and declines during the dry or harvest seasons. The process of vegetation growth and withering repeats through the crop cycles during the year. As a result, the NDVI growth trajectory attains the form of a harmonic wave over time in areas where multiple cropping cycles are practiced. The harmonic wave characteristics of the biomass change can be analyzed using the NDVI time series for the corresponding time period. We used the Fourier analysis technique to analyze the harmonic wave pattern of the NDVI curve.

Fourier analysis permits a complex curve to be expressed as the sum of a series of cosine waves (terms) and an additive term (Jakubauskas et al. 2001). The additive term represents the mean NDVI and each successive harmonic term explains a percentage of the total variance in the time series. High amplitude values for a given term indicate a high level of variation in temporal NDVI; the term in which that variation occurs indicates the periodicity of the event (Jakubauskas et al. 2001). The first harmonic term represents the annual cycle, the second harmonic term represents the biannual cycle, and so on. The prominence of one particular harmonic over others explains the cyclic nature of the curve. For example, if the amplitude of the second harmonic is higher than other harmonics, it indicates a strong biannual vegetation cycle in the time series. However, often, identification of the prominent harmonic is not straightforward. It is also dependent upon the amount of variance in original data that is contained in a specific harmonic term. Percent variance explained by each harmonic term can be computed by dividing the individual variance for each term by total variance (Jakubauskas et al. 2001).

A pixel-wise Fourier transformation of the time series for each MODIS scene was performed to produce the amplitude and phase images (Figures 7 and 8). Further, the number of crop cycles in each pixel was determined by identifying the dominant harmonic. The agricultural areas were classified into single-, double- or triple-crop areas.

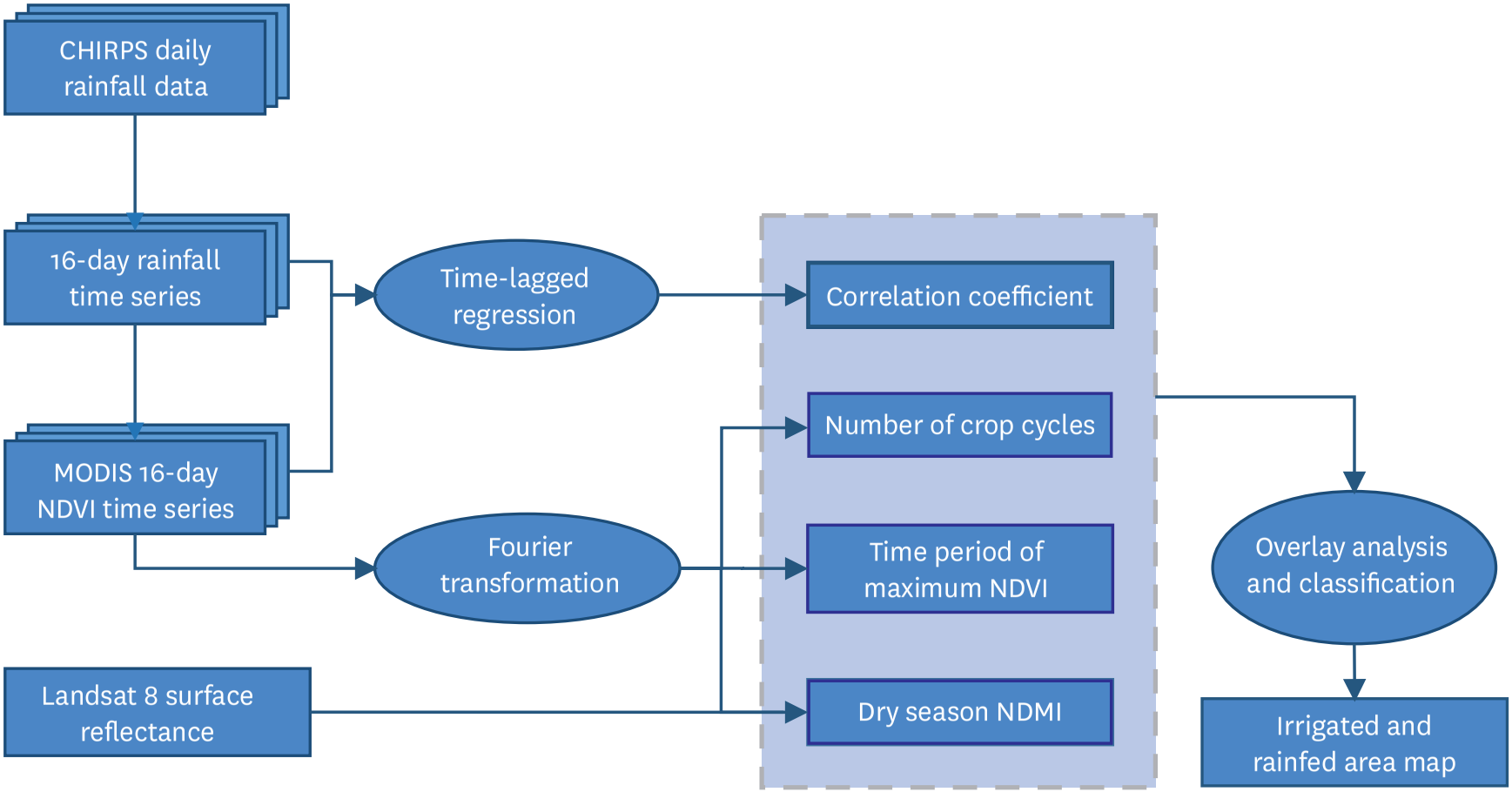

Figure 6. An overview of data inputs, variables defined and analytical methods used for identifying irrigated and rainfed areas in the agricultural areas of Ethiopia.

Notes: CHIRPS - Climate Hazards group InfraRed Precipitation with Stations; MODIS - Moderate Resolution Imaging Spectroradiometer; NDVI - Normalized Difference Vegetation Index; NDMI - Normalized Difference Moisture Index.

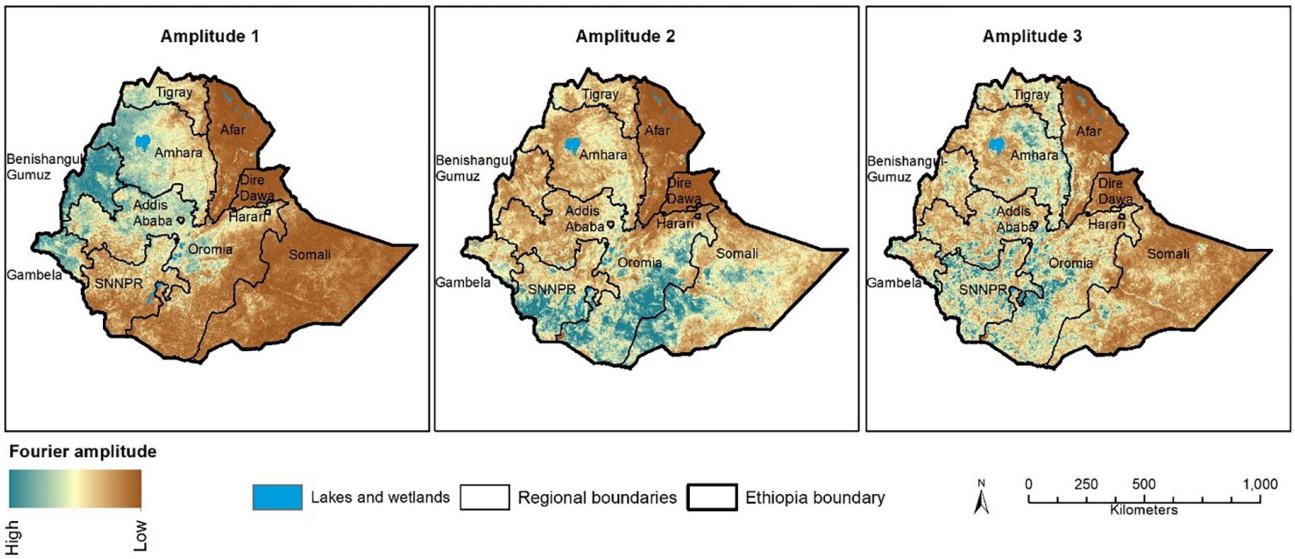

Figure 7. First three Fourier components of the annual time series NDVI.

Percent variance explained for each harmonic term was also computed on a per-pixel basis to assign a level of confidence for the single/double/triple crop categorization. Three confidence levels—high, medium and low—were assigned to the crop cycle classification. The NDVI profiles of the medium and low confidence areas were further manually explored to determine the number of crop cycles.

The Fourier analysis provides the approximate time period (phase) of the peak NDVI for each component. It was found that the phase value of the areas where two crop cycles are present can offer information for an initial separation between rainfed double crops and irrigated double crops. The phase angle value of the double-crop cycle in areas depends on the remaining moisture of the first crop or, in regions where a second rainfall season is present, is different from irrigated double-crop areas. The phase angle value of double-crop areas was explored to arrive at thresholds to separate rainfed double-crop and irrigated double-crop areas.

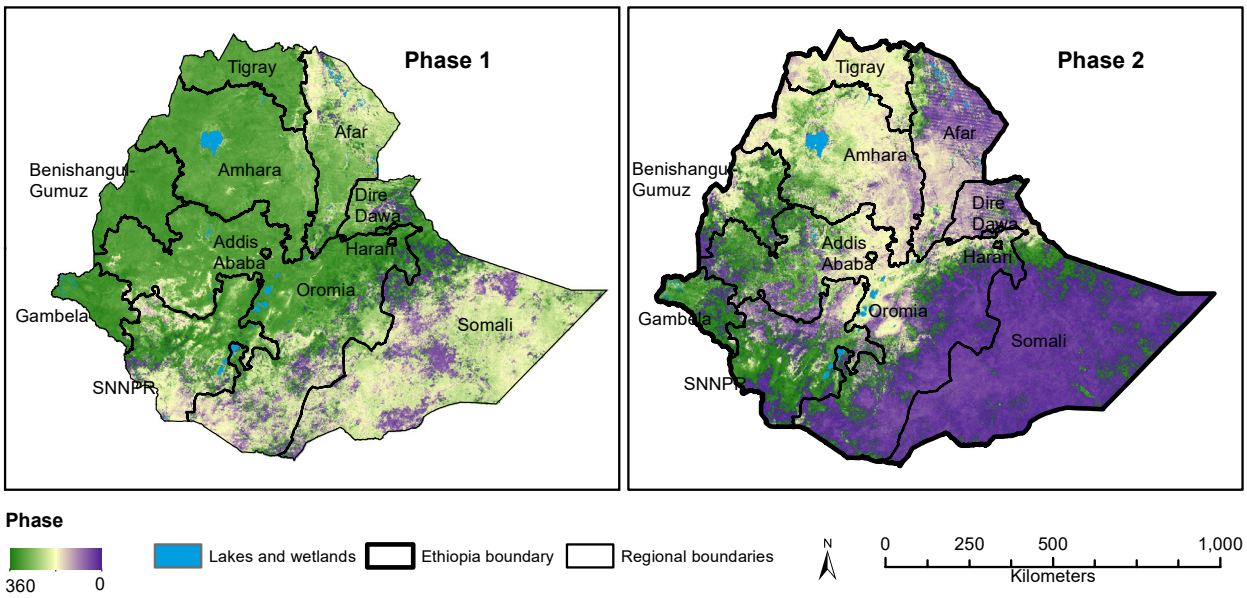

Figure 8. Phase images indicating the time period of the peaks in the first two Fourier amplitudes.

Time-lagged Regression

Since many areas in Ethiopia have more than one crop cycle depending on the remaining moisture of the first cropping season or the occurrence of a second rainfall season, the information on the number of crop cycles alone cannot be used as an identifier of irrigated areas. To determine whether an area is rainfed or irrigated, further information was required about the dependence of agriculture on rainfall.

The rainfall patterns affect the trends of plant growth in agriculture and other natural vegetation types. At the same time, the NDVI—rainfall trends (Figures 4 and 5) show that irrigated and rainfed areas exhibit varying levels of dependence on rainfall. Further analysis was focused on the quantification of the dependence of agriculture on rainfall. More specifically, the analysis was intended to explore the temporal relationship between the growth of green vegetation in croplands and the rainfall season. The analysis assumes that rainfed agriculture should have a strong positive correlation with the rainfall period, while the irrigated areas will have a weaker correlation. Other forms of water management should exhibit varying levels of correlation between these two extremes.

The temporal relationship between the intra-annual NDVI and rainfall time series was quantified using a time-lagged regression between these two data sets. Rainfall was considered as the independent variable and NDVI as the response variable. It has been observed that the vegetation response to rainfall has a time lag (Ji and Peters 2005), and therefore time-lagged regression was performed to assess this relationship. A time lag of one step in the time series (16 days) was used for the analysis, and the lagged correlation coefficient r was estimated for each pixel (Figure 9).

While the r values range from -0.92 to 0.96, the values of the agricultural areas range from -0.85 to 0.93. Broadly, the correlation estimates derived from the lagged regression demonstrate that the rainfed areas are positively correlated with rainfall and areas that show a high negative correlation are irrigated. Areas with various other forms of water management exhibited either low positive or low negative correlations. While this describes the general nature of the NDVI-rainfall relationship, it was observed that factors such as the presence of a large number of trees, period of cultivation, etc., also impact this relationship.

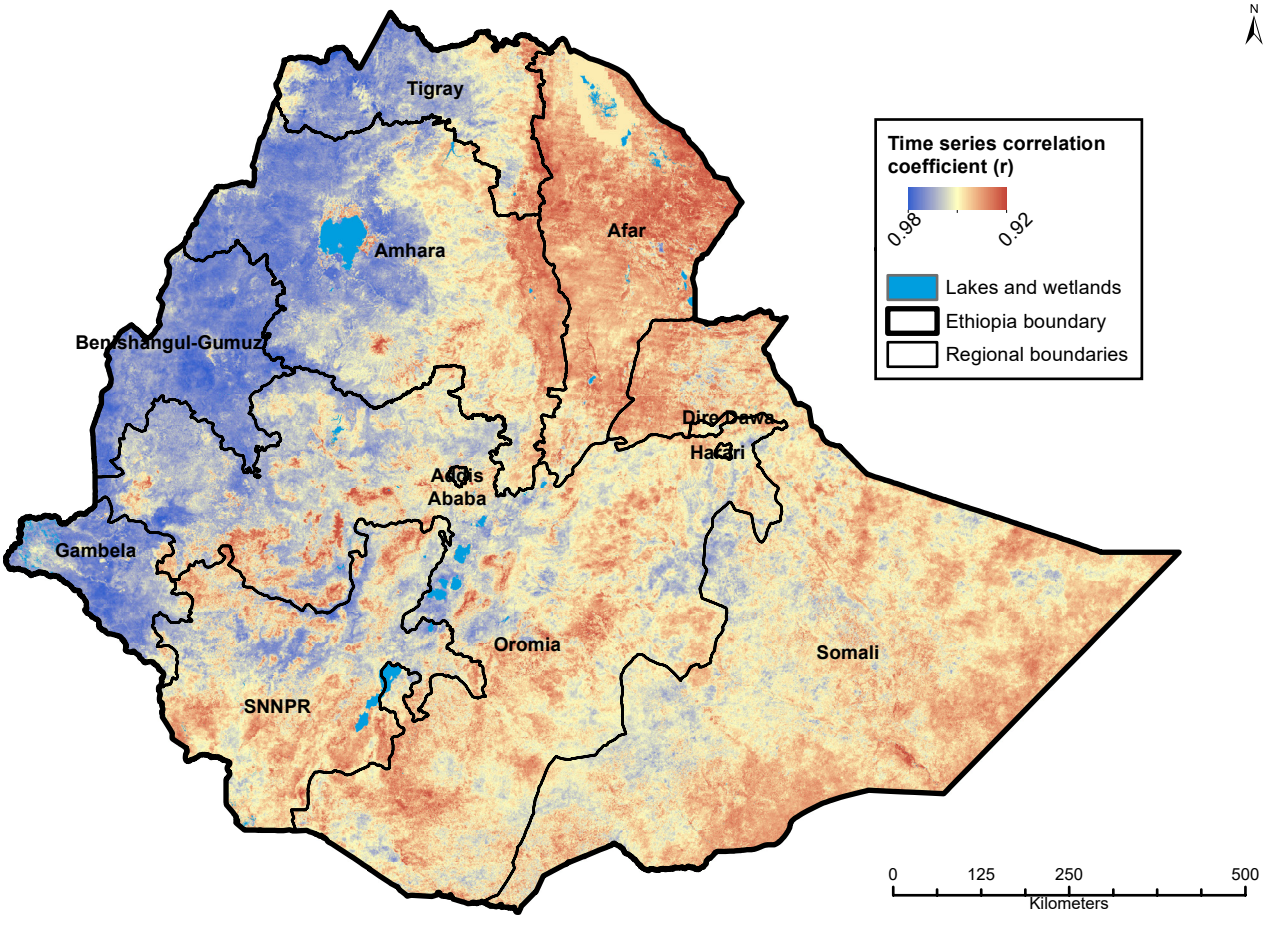

Figure 9. Time series correlation between annual rainfall time series and annual NDVI time series from April 2015 to March 2016.

Dry Season Moisture Status

Apart from supplementary irrigation and spate irrigation areas, most irrigated areas in Ethiopia receive irrigation during the dry season. Dry season moisture status in the croplands was identified as a potential variable to distinguish irrigated and rainfed areas. We used NDMI derived from Landsat 8 OLI/TIRS Surface Reflectance images to assess the moisture status.

During the dry season, most irrigated landscapes might have a higher level of moisture content compared to the rainfed areas, but this may not be true in the case of wetlands, riverbeds, valley bottoms and areas where various forms of water management exist. Additionally, the moisture levels estimated through satellite images may be affected by several factors such as the proximity of dates of images and the period of irrigation, variations in the intensity of irrigation, soil type, crop type, etc. As these factors have significant variability across the country and since there is no ground truth information available for moisture status, it was not possible to use this variable alone as a quantitative measure to enhance the classification. Therefore, NDMI was used as a complementary variable along with the measures derived through the seasonality analysis.

We used NDMI images from January 2016 for the analysis of moisture status. Wherever images from January were not available due to cloud cover, images from February 2016 were used for the NDMI calculation (Figure 10). Images from the other months had significant cloud cover and were thus not suitable for the analysis.

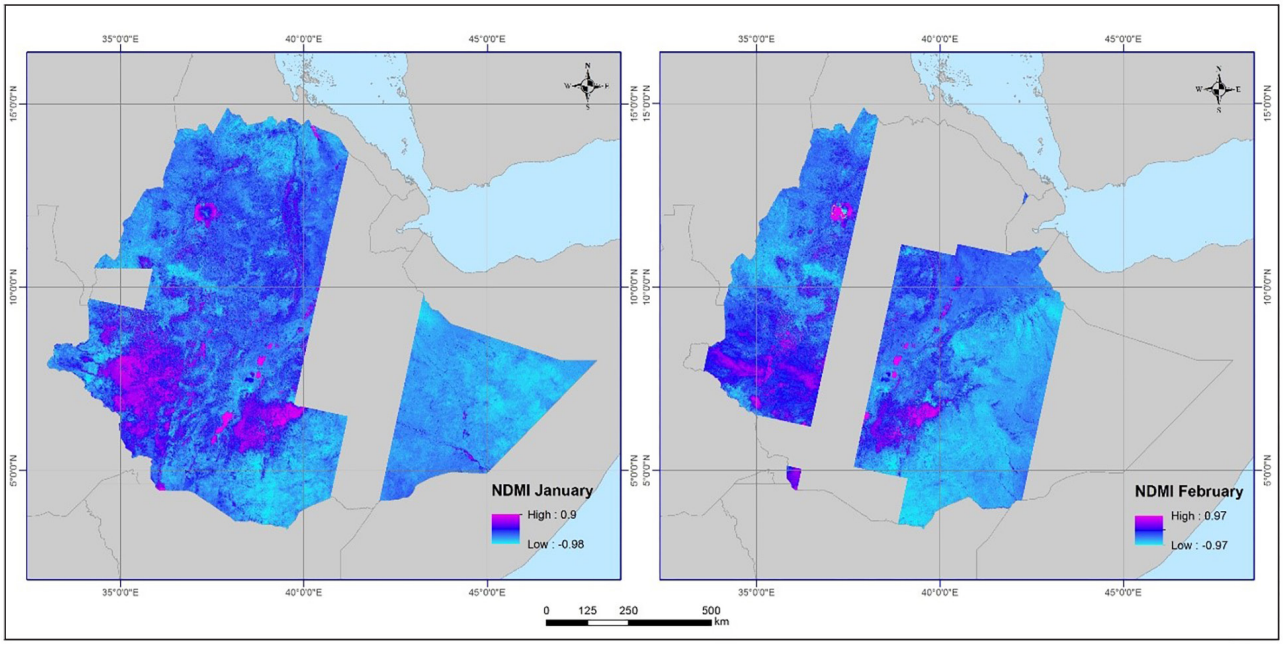

Figure 10. Normalized Difference Moisture Index (NDMI) of January and February 2016.

Overlay Analysis and Classification

The agricultural landscape was categorized by combining the following variables to describe crop cycles, landscape mixture, rainfall dependence and dry season moisture status.

- Time-lagged correlation between NDVI and rainfall time-series.
- Number of crop cycles.
- Time period of maximum NDVI for multiple crop cycles.
- Dry season NDMI derived from January or February images.
- The Landsat-based agricultural area map as a mask to exclude non-agricultural areas.

The classification was performed by developing suitable thresholds for each of these variables to ensure optimal separation of irrigated and rainfed categories. The available ground truth information and high-resolution images available in Google Earth were used extensively to explore a large number of pixels to develop these thresholds. Thresholds were identified regionally to account for the spatial variations in rainfall and irrigation patterns. The results were examined visually with ground truth data and Google Earth data, and thresholds were iteratively refined locally to improve the results. The individually categorized layers were combined through an overlay analysis. The outputs were visually compared with ground truth data, Landsat images and Google Earth data, and corrections were made to improve the results.

Accuracy Assessment

An ideal accuracy assessment procedure requires ground verification of randomly generated sample locations during the period from which images were used. Since such a data set was not generated for this study, we utilized existing secondary data sets obtained from the government departments and past studies described in the section *Data Sources*. A set of 1,100 points, which were not used in the classification process, were used for the validation of the final map. The points were selected after ensuring the suitability of the points for a pixel-to-pixel accuracy assessment, as described earlier. Only locations from irrigated areas were available for validation. Coordinates of rainfed areas were not available in this data set for the accuracy assessments. The proportion of the number of points correctly classified as irrigated was calculated to arrive at an estimation of the accuracy of the results.

Results and Discussion

The outcome is a map of agricultural areas of Ethiopia classified into irrigated and rainfed categories, with a pixel resolution of 30 m. As described in the section *Materials and Methods*, the crop area classification and irrigated area identification were performed in successive stages of the analysis. The results of each step are discussed below.

Crop Area Classification

The crop area map (Figure 11) is the result of a rapid classification of 59 Landsat 8 scenes using the cloud computing facilities offered by Google Earth Engine. The classification of agricultural areas requires the sampling of non-agricultural landscapes with sampling intensity similar to agricultural areas to exclude possible misclassification of these areas into agriculture. However, the focus of the analysis was to separate agriculture from various other land cover categories. Except for the agriculture class, all other land use categories were removed from the final map. The crop area map includes areas with standing crops, harvested crops and fallow lands that may not have been cultivated during the study year. The total area of croplands, including all these categories, is 21,845,290 ha (Table 2).

Irrigated Area Mapping

The analysis was performed using the images acquired between April 2015 and March 2016. The final map consists of the following two categories:

1. Irrigated agriculture: Includes areas with at least one crop cycle using irrigation as a water source.

2. Rainfed agriculture: Areas where water requirements are met directly from rainfall.

The crop area map was produced solely using the Landsat 8 images with 30 m resolution; the resolution of the final output also remains the same. The irrigated/rainfed area classification was performed using the crop area and NDMI layers with 30 m resolution and phenological variables with 250 m resolution. The final maps of agricultural area and irrigated/rainfed areas are produced at 30 m resolution (Figure 11 and 12).

The extent of irrigated and rainfed areas in different regional states is provided in Table 2. These statistics for zones and *woredas*[6] (districts) are provided in the Appendix.

[6] *Woreda* is the third-level administrative division of Ethiopia.

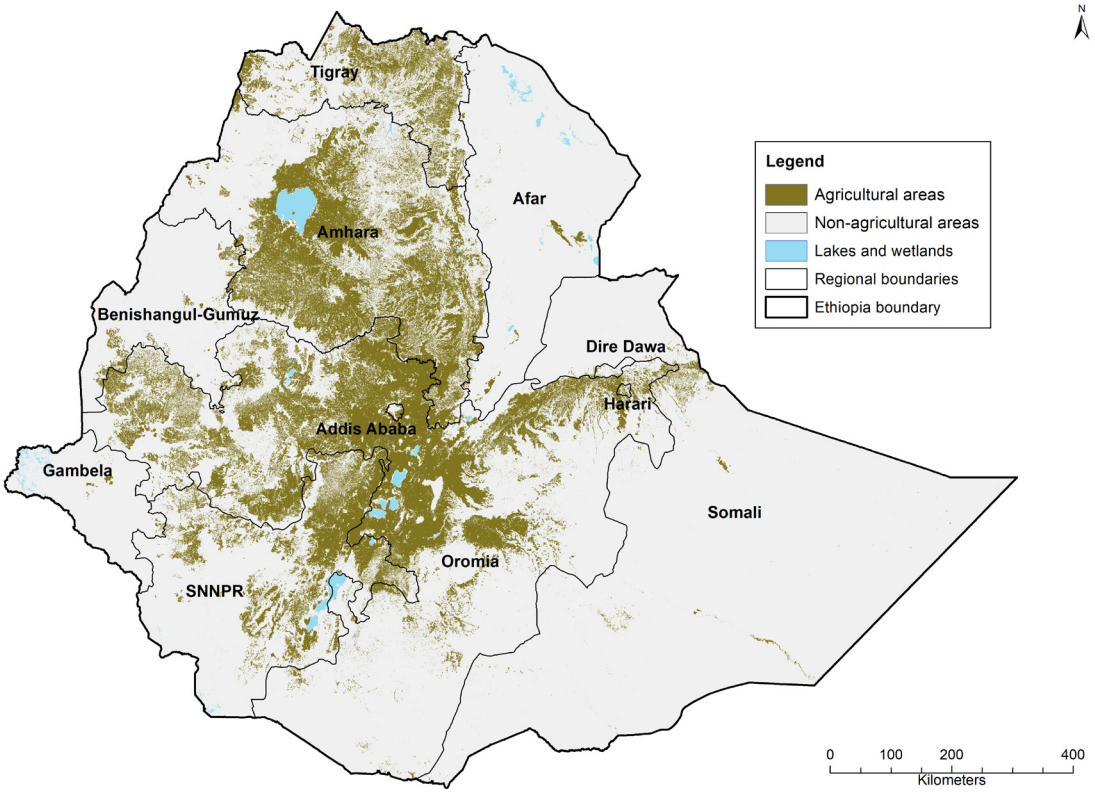

Figure 11. Agricultural areas in Ethiopia during the period 2015-2016 mapped at 30 x 30 m resolution. The crop areas also include fallow lands.

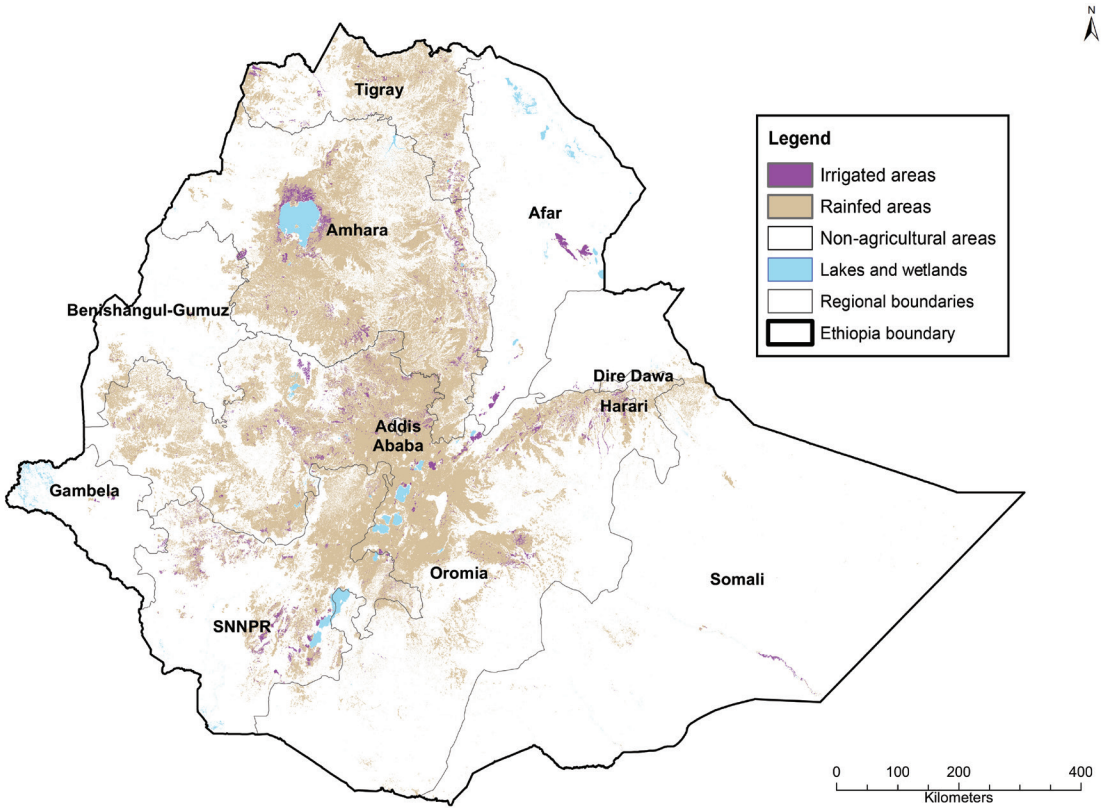

Figure 12. Map of irrigated and rainfed areas in Ethiopia during the period 2015-2016 mapped at 30 x 30 m resolution.

The results show that only around 5% of the estimated agricultural area in Ethiopia is under irrigation in 2015-2016. The total area under irrigation estimated by this study is approximately 1.11 Mha. The extent of rainfed agriculture was estimated at 20.7 Mha. The large regional states, such as Oromia and Amhara, have the largest areas under irrigation. Together, these two regions cover ~67% of the entire irrigated area in the country (Table 2). However, the percentage of irrigated areas within croplands is highest in Afar (63.2%), followed by Gambela (33.7%) (Figure 13). Afar region is characterized by an arid and semi-arid climate with low and erratic rainfall patterns (Melese et al. 2018). As a result, rainfed farming is not feasible in most areas of the region. On the other hand, the availability of water sources and private investments in commercial farms would have aided irrigated agriculture in Gambela (Degife et al. 2018).

The accuracy assessment of the results based on the GPS coordinates of the irrigated areas obtained from MoA shows an agreement of 70% with the classified output. The validation data set contains only irrigated area locations, and hence only the error of omission (exclusion) could be estimated from these data. Since the MODIS NDVI data have a relatively coarse pixel resolution of 250 m, it is likely to include multiple land cover types in many areas. This has been observed as being a major contribution to errors in area estimation using coarse resolution mapping. By combining the Landsat-derived NDMI with a pixel resolution of 30 m, the results were spatially better refined.

Table 2. Area of irrigated and rainfed agriculture in different regions of Ethiopia.

Region	Area (hectares)		
	Irrigated agriculture	Rainfed agriculture	Agricultural area
Addis Ababa	507	24,700	25,207
Afar	72,835	42,339	115,174
Amhara	315,356	6,449,491	6,764,847
Benishangul- Gumuz	6,212	236,414	242,626
Dire Dawa	1,722	8,479	10,201
Gambela	9,880	19,458	29,338
Harari	2,542	15,133	17,675
Oromia	428,026	9,539,555	9,967,581
SNNPR	195,028	2,563,431	2,758,459
Somali	18,567	241,927	260,494
Tigray	59,753	1,593,935	1,653,688
Total area	1,110,428	20,734,862	21,845,290

Note: SNNPR - Southern Nations, Nationalities, and People's Region.

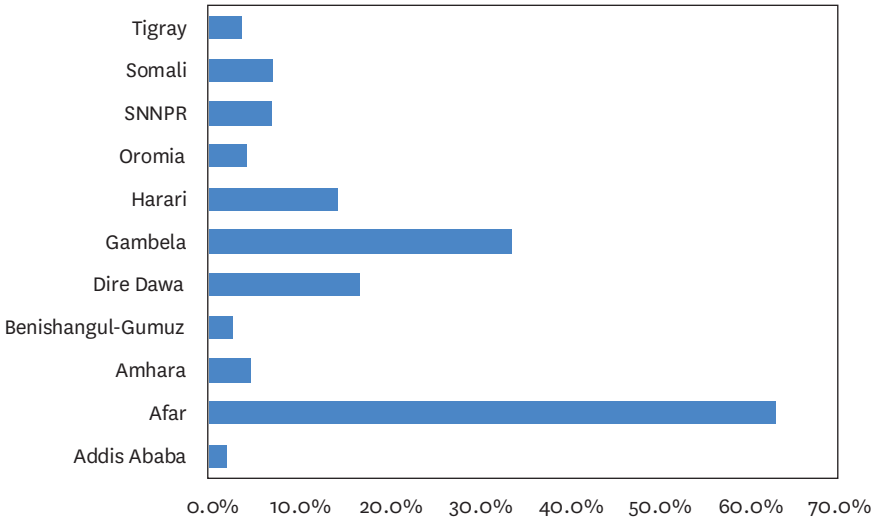

Figure 13. Percentage of irrigated areas within agricultural areas in the regional states.
Note: SNNPR - Southern Nations, Nationalities, and People's Region.

Comparison of the Results with Other Estimates

The total crop area estimated by this study is 21.8 Mha, which is close to a recent estimate of 18.1 Mha by government agencies (CSA 2018). Considerable variations exist in the irrigated area estimations of Ethiopia reported by different sources. MoWIE (2018) highlights some of these differences in estimations by various government agencies - the irrigated area estimate according to the Ministry of Agriculture and Natural Resources (MoANR) and the Ministry of Water, Irrigation and Energy (MoWIE) is 2.94 Mha, while it is 1.58 Mha according to the data from various Regional Bureaus of Irrigation and MoWIE. A fresh assessment presented in MoWIE (2018) estimates the total irrigated area as 1.65 Mha, which was calculated using digitized Google Earth images and data from reports of regional agencies. As mentioned earlier, this study estimates the total irrigated area as 1.11 Mha. A comparison of the region-wise results of MoWIE (2018) and this study is presented in Table 3. The major difference between these studies is in Oromia, followed by Somali region. This study reports the irrigated area of Oromia to be 428,026 ha, while MoWIE (2018) provides a much higher estimate of 756,578 ha. However, another recent report by the Oromia Irrigation Development Authority (OIDA) estimates the irrigated area in the Oromia region as 351,129 ha (OIDA 2018). The study conducted by OIDA (2018) used secondary data from district-level agencies, information collected from key stakeholders and partial site visits, and Google Earth images. The estimate of this study is much closer to that of OIDA (2018), which is based on a more detailed inventory. Secondary data from a similar inventory of the irrigated sites in Tigray by MoA show the irrigated area extent as 50,083 ha, whereas this study estimates the area as 59,753 ha. Overall, the irrigated area estimates of this study broadly confirm the MoA estimations.

Limitations of the Study

One of the limitations of this study is the possibility of limited success in identifying isolated small-scale irrigated plots. Even though one of the variables (NDMI) used for the analysis has a resolution of 30 m, the seasonality variables derived from the MODIS data have a pixel size of ~6.25 ha. The coarse pixel size may result in mixed pixels, including various land cover types in many areas, and this might have had an impact on the regression analysis. In a pixel-based classification, the pixels are generally allocated to the dominant land cover category present within the pixel. Therefore, any irrigated area which occupies a minor portion of the MODIS pixel needs to be identified only with a single variable—dry season NDMI. As described in the section *Dry Season Moisture Status*, NDMI alone would not be sufficient to identify irrigated areas because of the variations in moisture levels due to several factors, such as crop type, irrigation intensity, rainfall period, etc. The effect of mixed pixels can be reduced by utilizing higher resolution images. However, the availability of cloud-free, multi-spectral imagery required for the time series analysis is limited in most areas of Ethiopia. It may be worth considering the synthetic aperture radar (SAR) images, such as Sentinel 1 data, to develop the crop growth profiles.

Another limitation might be distinguishing areas with high soil moisture such as wetlands and valley bottoms from irrigated areas. These areas, with an abundance of soil moisture, are likely to show less dependence on rainfall for the crop growing season, and might exhibit similar crop growing and moisture patterns of irrigated areas. Integrating a map of wetlands and valley bottoms, and developing separate thresholds for analysis of these regions might help to improve the results in such areas.

The intra-annual rainfall time series derived from the CHIRPS rainfall product is one of the most important data sets used for the analysis. The results of the time series regression particularly rely upon the accuracy of rainfall estimates in the CHIRPS data product. While the CHIRPS data can replicate rainfall patterns reasonably well, it may have certain performance issues in higher elevation areas (Kimani et al. 2017).

Table 3. Comparison of region-wise irrigated area estimations of this study and a recent report by the Ministry of Water, Irrigation and Energy (MoWIE), Ethiopia.

Region	Irrigated agricultural area (hectares)	
	This study	MoWIE (2018)
Addis Ababa	507	406
Afar	72,835	72,525
Amhara	315,356	375,193
Benishangul-Gumuz	6,212	34,684
Dire Dawa	1,722	3,070
Gambela	9,880	28,407
Harari	2,542	3,106
Oromia	428,026	756,578
SNNPR	195,028	198,873
Somali	18,567	109,908
Tigray	59,753	69,901
Total area	1,110,428	1,652,651

Conclusions

This study presents the results of remote sensing-based mapping and area estimations of the irrigated and rainfed areas of Ethiopia in 2015-2016. Irrigated areas are mapped by analyzing the temporal relationship between remotely sensed vegetation and rainfall data sets and dry season moisture status estimated using remote sensing data. The results indicate that irrigated areas in this region can be identified reasonably well by analyzing seasonal variations in biomass and moisture levels.

While the analysis was reasonably successful in identifying irrigated and rainfed areas, improvements are required in identifying isolated small-scale irrigated areas, and the separation of irrigated areas and soil moisture-based cultivations in wetlands and valley bottoms. It must also be noted that the ground truth points used for validation only include irrigated areas. Better quantification of uncertainties may be achieved using more representative sample data sets such as rainfed area coordinates for validation, if available.

The study estimates that an area of approximately 1.11 Mha is currently irrigated, which is only around 5% of the total agricultural area in Ethiopia. These results broadly confirm the available regional estimates of irrigated area extent by government agencies. Except for Afar and Gambela, all other regional states have a very small percentage of croplands under irrigation (< 10%). The high dependency on rainfed farming makes the food security of the region vulnerable to rainfall variability. The results of this study provide important information about the spatial extent and distribution of existing irrigated areas. The methodology presented here could be used for future monitoring of irrigation development in the country. A detailed irrigation suitability analysis combined with these results will provide valuable information for policy makers, decision-makers and investors about future irrigation development in Ethiopia.

References

Breiman, L. 2001. Random forests. *Machine Learning* 45(1): 5–32. https://doi.org/10.1023/A:1010933404324

Breiman, L.; Friedman, J.H.; Olshen, R.A.; Stone, C.J. 1984. *Classification and regression trees*. New York: Chapman and Hall. 358p.

Chandrasekharan, K.; Cai, X.; Siddiqui, S.; Rajah, A.; Subasinghe, S. 2015. Irrigated and rainfed area map of Africa, 2010-2011. Data set. IWMI Water Data Portal. Colombo, Sri Lanka: International Water Management Institute. Available at http://waterdata.iwmi.org/applications/irri_area/ (accessed January 19, 2017).

CSA (Central Statistical Agency). 2018. *Key findings of the 2017/2018 (2010 E.C.) agricultural sample surveys*. Addis Ababa, Ethiopia: Central Statistical Agency, Federal Democratic Republic of Ethiopia.

Dahal, D.; Wylie, B.; Howard, D. 2018. Rapid crop cover mapping for the coterminous United States. *Scientific Reports* 8: 8631. https://doi.org/10.1038/s41598-018-26284-w

Degife, A.W.; Zabel, F.; Mauser, W. 2018. Assessing land use and land cover changes and agricultural farmland expansions in Gambella region, Ethiopia, using Landsat 5 and Sentinel 2a multispectral data. *Heliyon* 4(11): e00919. https://doi.org/10.1016/j.heliyon.2018.e00919

Didan, K. 2015. MOD13Q1 MODIS/Terra vegetation indices 16-Day L3 global 250 m SIN grid V006. Data set. Distributed by NASA EOSDIS Land Processes DAAC. Available at https://doi.org/10.5067/MODIS/MOD13Q1.006 (accessed January 11, 2021).

FAO (Food and Agriculture Organization of the United Nations). 2016. AQUASTAT database: Global map of irrigated area - Ethiopia. Rome, Italy: Food and Agriculture Organization of the United Nations (FAO). Available at http://www.fao.org/aquastat/en/geospatial-information/global-maps-irrigated-areas/irrigation-by-country/country/ETH (accessed April 7, 2021).

Funk, C.; Peterson, P.; Landsfeld, M.; Pedreros, D.; Verdin, J.; Shukla, S.; Husak, G.; Rowland, J.; Harrison, L.; Hoell, A.; Michaelsen, J. 2015. The climate hazards infrared precipitation with stations—a new environmental record for monitoring extremes. *Scientific Data* 2:150066. https://doi.org/10.1038/sdata.2015.66

Google Earth Engine. 2017. Landsat 8 8-day TOA reflectance composite. Data set. California, USA: Google Inc. Available at https://explorer.earthengine.google.com/#detail/LANDSAT%2FLC8_L1T_8DAY_TOA (accessed January 10, 2017).

Haile, G.G.; Kassa, A.K. 2015. Irrigation in Ethiopia: A review. *Academia Journal of Agricultural Research* 3(10): 264–269.

Huete, A.; Didan, K.; Miura, T.; Rodriguez, E.P.; Gao, X.; Ferreira L.G. 2002. Overview of the radiometric and biophysical performance of the MODIS vegetation indices. *Remote Sensing of Environment* 83(1–2): 195–213. https://doi.org/10.1016/S0034-4257(02)00096-2

Iverson, L.R.; Prasad, A.M.; Matthews, S.N.; Peters, M. 2008. Estimating potential habitat for 134 eastern US tree species under six climate scenarios. Forest *Ecology and Management* 254: 390–406.

Jakubauskas, M.E.; Legates, D.R.; Kastens, J.H. 2001. Harmonic analysis of time-series AVHRR NDVI data. *Photogrammetric Engineering & Remote Sensing* 67(4): 461–470.

Ji, L.; Peters, A.J. 2005. Lag and seasonality considerations in evaluating AVHRR NDVI response to precipitation. *Photogrammetric Engineering and Remote Sensing* 71(9): 1053–1061. https://doi.org/10.14358/PERS.71.9.1053

Kimani, M.W.; Hoedjes, J.C.B.; Su, Z. 2017. An assessment of satellite-derived rainfall products relative to ground observations over East Africa. *Remote Sensing* 9(5): 430. https://doi.org/10.3390/rs9050430

Krishnaswamy, J.; Kiran, M.C.; Ganeshaiah, K.N. 2004. Tree model based eco-climatic vegetation classification and fuzzy mapping in diverse tropical deciduous ecosystems using multi-season NDVI. *International Journal of Remote Sensing* 25(6): 1185–1205. https://doi.org/10.1080/01431160310000149989

Lyon, J.G.; Yuan, D.; Lunetta, R.S.; Elvidge, C.D. 1998. A change detection experiment using vegetation indices. *Photogrammetric Engineering and Remote Sensing* 64(2): 143–150.

Matsushita, B.; Yang, W.; Chen, J.; Onda, Y.; Qiu, G. 2007. Sensitivity of the Enhanced Vegetation Index (EVI) and Normalized Difference Vegetation Index (NDVI) to topographic effects: A case study in high-density cypress forest. *Sensors* 7(11): 2636–2651. https://doi.org/10.3390/s7112636

Melese, A.; Suryabhagavan, K.V.; Balakrishnan, M. 2018. Multi-model and vegetation indices for drought vulnerability assessment: A case study of Afar region in Ethiopia. *Remote Sensing of Land* 2(1): 1–14. https://doi.org/10.21523/gcj1.18020101

Morton, R.D.; Rowland, C.S. 2015. *Developing and evaluating an Earth observation-enabled ecological land cover time series system*. JNCC Report No 563. Peterborough, UK: Joint Nature Conservation Committee.

MoWIE (Ministry of Water, Irrigation and Energy). 2018. Assessment of national water used and demand forecast. In: *Part II – Water uses and demand forecast*. Addis Ababa, Ethiopia: Ministry of Water, Irrigation and Energy, Federal Democratic Republic of Ethiopia. Unpublished.

NASA JPL (National Aeronautics and Space Administration Jet Propulsion Laboratory). 2013. NASA Shuttle Radar Topography Mission global 1 arc second. Data set. Distributed by NASA EOSDIS Land Processes DAAC. Available at https://doi.org/10.5067/MEaSUREs/SRTM/SRTMGL1.003 (accessed January 11, 2021).

Naser, M.A.; Khosla, R.; Longchamps, L.; Dahal, S. 2020. Using NDVI to differentiate wheat genotypes productivity under dryland and irrigated conditions. *Remote Sensing* 12(5): 824. https://doi.org/10.3390/rs12050824

OIDA (Oromia Irrigation Development Authority). 2018. *Oromia irrigation potential assessment project: List of identified scheme inventory report (draft)*. Addis Ababa, Ethiopia: Oromia Irrigation Development Authority.

Ouma, Y.O.; Tateishi, R. 2008. Urban-trees extraction from Quickbird imagery using multiscale *spectex*-filtering and non-parametric classification. *ISPRS Journal of Photogrammetry and Remote Sensing* 63(3): 333–351. https://doi.org/10.1016/j.isprsjprs.2007.10.006

Pervez, M.S.; Budde, M.; Rowland, J. 2014. Mapping irrigated areas in Afghanistan over the past decade using MODIS NDVI. *Remote Sensing of Environment* 149: 155–165. https://doi.org/10.1016/j.rse.2014.04.008

Pun, M.; Mutiibwa, D.; Li, R. 2017. Land use classification: A surface energy balance and vegetation index application to map and monitor irrigated lands. *Remote Sensing* 9(12): 1256. https://doi.org/10.3390/rs9121256

Schmitter, P.; Kibert, K.S.; Lefore, N.; Barron, J. 2018. Suitability mapping framework for solar photovoltaic pumps for smallholder farmers in sub-Saharan Africa. *Applied Geography* 94: 41–57. https://doi.org/10.1016/j.apgeog.2018.02.008

Senf, C.; Leitão, P.J.; Pflugmacher, D.; van der Linden, S.; Hostert, P. 2015. Mapping land cover in complex Mediterranean landscapes using Landsat: Improved classification accuracies from integrating multi-seasonal and synthetic imagery. *Remote Sensing of Environment*. 156: 527–536. https://doi.org/10.1016/j.rse.2014.10.018

Siebert, S.; Henrich, V.; Frenken, K.; Burke, J. 2013a. Global map of irrigation areas, version 5. Bonn, Germany: Rheinische Friedrich-Wilhelms-University; Rome, Italy: Food and Agriculture Organization of the United Nations (FAO). http://www.fao.org/aquastat/en/geospatial-information/global-maps-irrigated-areas/latest-version (accessed April 7, 2021).

Siebert, S.; Henrich, V.; Frenken, K.; Burke, J. 2013b. Update of the digital global map of irrigation areas to version 5. Bonn, Germany: Rheinische Friedrich-Wilhelms-University/ Rome, Italy: Food and Agriculture Organization of the United Nations. http://www.fao.org/3/I9261EN/i9261en.pdf (accessed April 7, 2021).

Thenkabail, P.S.; Biradar, C.M.; Noojipady, P.; Dheeravath, V.; Li, Y.J.; Velpuri, N.M.; Gumma, M.K.; Gangalakunta, O.R.P.; Turral, H.; Cai, X.; Vithanage, J.; Schull, M.A.; Dutta, R. 2009. Global irrigated area map (GIAM), derived from remote sensing, for the end of the last Millennium. *International Journal of Remote Sensing* 30(14): 3679–3733. https://doi.org/10.1080/01431160802698919

Thenkabail, P.S.; Wu, Z. 2012. An automated cropland classification algorithm (ACCA) for Tajikistan by combining Landsat, MODIS, and secondary data. *Remote Sensing* 4(10): 2890–2918. https://doi.org/10.3390/rs4102890

USGS (United States Geological Survey). 2016. *Product guide: Landsat surface reflectance derived spectral indices, version 3.0*. Department of the Interior, U.S. Geological Survey.

Wardlow, B.D.; Egbert, S.L.; Kastens, J.H. 2007. *Analysis of time-series MODIS 250 m vegetation index data for crop classification in the U.S. Central Great Plains*. Lincoln, USA: University of Nebraska. (Drought Mitigation Center Faculty Publications). Available at https://digitalcommons.unl.edu/droughtfacpub/2 (accessed January 12, 2021).

Welteji, D. 2018. A critical review of rural development policy of Ethiopia: Access, utilization and coverage. *Agriculture & Food Security* 7: 55. https://doi.org/10.1186/s40066-018-0208-y

Wilson, E.H.; Sader, S.A. 2002. Detection of forest harvest type using multiple dates of Landsat TM imagery. *Remote Sensing of Environment* 80(3): 385–396. https://doi.org/10.1016/S0034-4257(01)00318-2

Worqlul, A.W.; Jeong, J.; Dile, Y.T.; Osorio, J.; Schmitter, P.; Gerik, T.; Srinivasan, R.; Clark, N. 2017. Assessing potential land suitable for surface irrigation using groundwater in Ethiopia. *Applied Geography* 85: 1–13. https://doi.org/10.1016/j.apgeog.2017.05.010

You, X.; Meng, J.; Zhang, M.; Dong, T. 2013. Remote sensing based detection of crop phenology for agricultural zones in China using a new threshold method. *Remote Sensing* 5(7): 3190–3211. https://doi.org/10.3390/rs5073190

Appendix. Subnational statistics of irrigated areas.

Table A1. Zone-wise area of irrigated and rainfed crops in Ethiopia (2015-2016).

Regional state	Zone	Area (hectares)	
		Irrigated crops	Rainfed crops
Addis Ababa	Region 14	507	24,700
Afar	Zone 1	50,919	5,918
	Zone 2	703	4,731
	Zone 3	20,775	20,003
	Zone 4	24	6,643
	Zone 5	414	5,044
Amhara	Agew Awi	14,227	374,647
	East Gojam	31,662	811,142
	North Gonder	90,902	911,715
	North Shewa (R3)	28,184	1,000,128
	North Wollo	34,208	461,500
	Oromia	7,892	125,220
	South Gonder	36,149	809,085
	South Wollo	28,916	896,471
	Special *Woreda*	714	5,732
	Wag Himra	467	199,110
	West Gojam	42,035	854,741
Benishangul-Gumuz	Asosa	1,395	114,352
	Kamashi	156	33,720
	Metekel	4,661	88,342
Dire Dawa	Dire Dawa	1,722	8,479
Gambela	Anuak	5,778	18,693
	Mezhenger	4,100	664
	Nuer	2	101
Harari	Harari	2,542	15,133
Oromia	Arsi	20,391	1,178,022
	Bale	39,445	746,438
	Borana	921	95,654
	East Hararghe	44,711	505,343
	East Shewa	48,968	652,863
	East Wellega	16,542	409,622
	Guji	736	167,775
	Horo Guduru Welega	19,524	270,782
	Ilubabor	1,516	425,149
	Jimma	15,018	741,054
	Kelam Wellega	6,084	279,249
	North Shewa (R4)	53,021	868,123
	South West Shewa	12,964	533,871
	West Arsi	7,754	716,615
	West Hararghe	36,137	584,182
	West Shewa	97,892	868,678
	West Wellega	6,402	496,135

(Continued)

Table A1. Zone-wise area of irrigated and rainfed crops in Ethiopia (2015-2016). (continued)

Regional state	Zone	Area (hectares)	
		Irrigated crops	Rainfed crops
SNNPR	Alaba	4	76,436
	Amaro	2,115	21,190
	Basketo	-	11,798
	Bench Maji	18,555	92,500
	Burji	2,066	23,720
	Dawro	4,607	76,611
	Derashe	13,196	41,904
	Gamo Gofa	50,519	294,148
	Gedio	353	7,585
	Gurage	4,360	331,380
	Hadiya	91	236,314
	Kembata Tembaro	2,638	108,132
	Keffa	45,222	199,494
	Konso	6,778	56,394
	Konta	1,362	14,945
	Selti	997	201,441
	Sheka	1,914	26,423
	Sidama	13,327	325,330
	South Omo	24,660	121,209
	Wolayita	774	266,311
	Yem	1,490	30,166
Somali	Afder	1,234	24,062
	Degehabur	5	15,033
	Fik	-	5,140
	Gode	14,725	7,136
	Jijiga	109	169,924
	Korahe	8	148
	Liben	275	7,572
	Shinile	2,211	11,318
	Warder	-	1,594
Tigray	Central	5,719	456,365
	Eastern	4,428	234,663
	Northwestern	5,758	334,501
	Southern	24,607	360,604
	Western	19,241	207,802
Total area		1,110,428	20,734,862

IWMI Working Paper Series

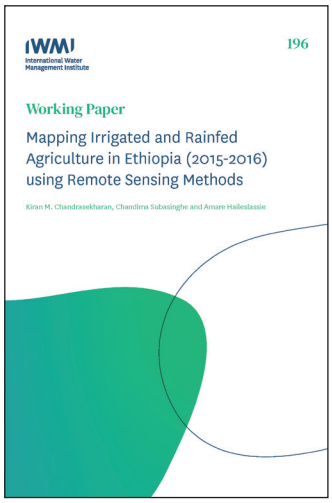

196 Mapping Irrigated and Rainfed Agriculture in Ethiopia (2015-2016) using Remote Sensing Methods
https://doi.org/10.5337/2021.206

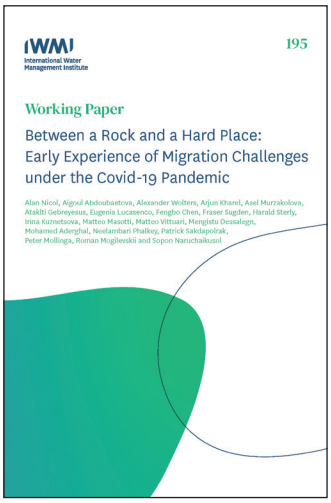

195 Between a Rock and a Hard Place: Early Experience of Migration Challenges under the Covid-19 Pandemic
https://doi.org/10.5337/2020.216

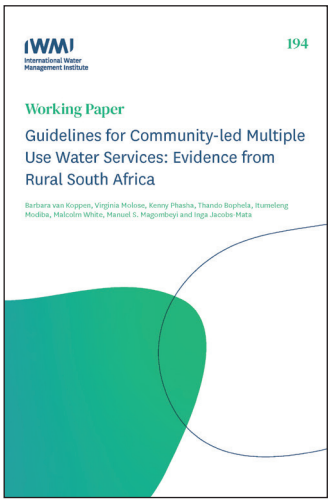

194 Guidelines for Community-led Multiple Use Water Services: Evidence from Rural South Africa
https://doi.org/10.5337/2020.213

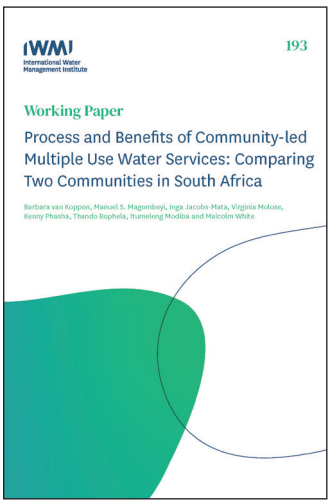

193 Process and Benefits of Community-led Multiple use Water Services: Comparing Two Communities in South Africa
https://doi.org/10.5337/2020.212

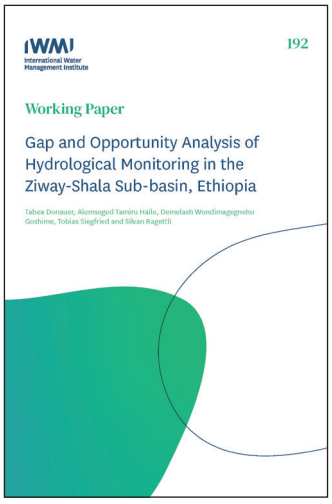

192 Gap and Opportunity Analysis of Hydrological Monitoring in the Ziway-Shala Sub-basin, Ethiopia
https://doi.org/10.5337/2020.210

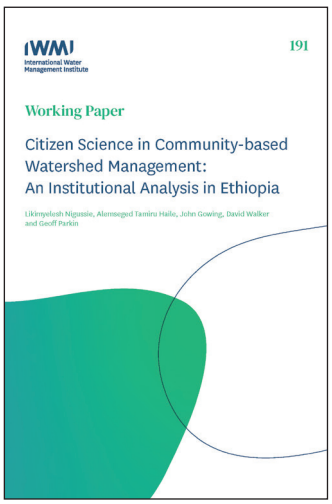

191 Citizen Science in Community-based Watershed Management: An Institutional Analysis in Ethiopia
https://doi.org/10.5337/2020.207

For access to all IWMI publications, visit: www.iwmi.org/publications/

Headquarters
127 Sunil Mawatha
Pelawatta
Battaramulla
Sri Lanka

Mailing address
P. O. Box 2075
Colombo
Sri Lanka

Telephone
+94 11 2880000

Fax
+94 11 2786854

Email
iwmi@cgiar.org

Website
www.iwmi.org

IWMI
International Water Management Institute

CGIAR
IWMI is a CGIAR Research Center

ISSN 2012-5763
e-ISSN 2478-1134
ISBN 978-92-9090-913-2